Mineralogy and Petrology (1998) 64: 187–218

Mineralogy and Petrology



# Iron-formations and epigenetic ironstones in the Palaeoproterozoic Willyama Supergroup, Olary Domain, South Australia

**P. M. Ashley**[1], **B. G. Lottermoser**[2], and **J. M. Westaway**[1,*]

[1] Division of Earth Sciences, University of New England, Armidale, Australia
[2] School of Earth Sciences, James Cook University, Cairns, Australia

With 10 Figures

Received December 3, 1997;
accepted July 24, 1998

**Summary**

Iron-formations occur as massive to compositionally layered, Fe oxide-rich, concordant bodies in the Palaeoproterozoic Willyama Supergroup of the Olary Domain, South Australia. They have constitutional similarities to those occurring in the neighbouring Broken Hill Domain. The most abundant iron-formations are in the Quartzofeldspathic Suite and comprise magnetite-quartz assemblages (± hematite, barite, actinolite, apatite). Hematite, magnetite, albite, quartz, Ca(Na) amphibole(s), CaNaFe clinopyroxene and andraditic garnet are major constituents of rare calc-silicate iron-formations in the Bimba and Calcsilicate Suites, whereas magnetite, quartz, almandine-spessartine, manganoan fayalite, manganoan grunerite and apatite form manganiferous iron-formations in the Pelite Suite. The pronounced differences in mineralogy of the three iron-formation types are the result of regional metamorphism of diverse hydrothermal precipitates with variable clastic components, together with the local effects of high-temperature metasomatic alteration. Metasomatic fluids were produced as a result of devolatilisation of the evaporite-bearing volcanosedimentary sequence, during and following amphibolite grade metamorphism and deformation, which led to localised and regional-scale hydrothermal alteration. In places, there was extensive metasomatic reconstitution (veining, brecciation, replacement) of iron-formations and associated rocks, caused by high-temperature (350°–650 °C), oxidising, saline fluids. The resulting epigenetic ironstones are dominated by magnetite-hematite-quartz with minor sulfides and display enrichment in Fe, Ti, Cu, Au, Sc, U, V, Y, Zn and HREE relative to parental iron-formations.

* Present address: Sons of Gwalia Limited, West Perth, Australia

**Zusammenfassung**

*Eisenformationen und epigenetische Eisensteine in der paläoproterozoischen Willyama Supergroup, Olary Domäne, Südaustralien*

Eisenformationen kommen als massige bis in der Zusammensetzung geschichtete, Eisenoxidreiche, konkordante Körper in der paläoproterozoischen Willyama Supergroup der Olary Domäne, Südaustralien, vor. Sie haben konstitutionelle Ähnlichkeiten mit Vorkommen in der benachbarten Broken Hill Domäne. Die häufigsten Eisenformationen befinden sich in der Quartzofeldspathic Suite and bestehen aus Magnetit und Quarz (± Hämatit, Baryt, Aktinolit, Apatit). Hämatit, Magnetit, Albit, Quarz, Ca(Na) Amphibol(e), CaNaFe Klinopyroxen und andraditischer Granat sind Hauptbestandteile von seltenen Kalksilikat-Eisenformationen in den Bimba und Calcsilicate Suites, während Magnetit, Quartz, Almandin-Spessartin, manganhaltiger Fayalit, manganhaltiger Grunerit und Apatit manganhaltige Eisenformationen in der Pelite Suite bilden. Die ausgeprägten Unterschiede in der Mineralogie der drei Typen von Eisenformationen sind durch Regionalmetamorphose von diversen hydrothermalen Ausfällungen mit variablen klastischen Komponenten verursacht worden, zusammen mit lokalen Wirkungen einer hock-Temperatur metasomatischen Alteration. Metasomatische Fluide wurden während und nach der Amphibolitmetamorphose und Deformation durch Devolatilisation der evaporithaltigen vulkanosedimentären Abfolge produziert, die sowohl zu lokaler, wie auch zu weiträumiger hydrothermaler Alteration führten. Örtlich kam es zu umfangreicher metasomatischer Rekonstitution (Gangbildung, Brekkzierung, Verdrängung) von Eisenformationen und assoziierten Gesteinen verursacht durch hoch-Temperatur (350°–650 °C), oxidierte, saline Fluide. Die resultierenden epigenetischen Eisensteine bestehen hauptsächlich aus Magnetit, Hämatit und Quarz mit Sulfiden und weisen eine Anreicherung in Fe, Ti, Cu, Au, Sc, U, V, Y, Zn und SREE relativ gegenüber den ursprünglichen Eisenformationen auf.

## Introduction

Proterozoic terranes typically contain iron-formations and ironstones as distinctive minor rock types. Iron-formations are characterised by sedimentary banding and a simple quartz and Fe oxide (magnetite and/or hematite) assemblage, but may grade into silicate or carbonate facies types and also contain variable amounts of other phases including sulfates, sulfides or phosphates. The geochemical composition of iron-formations is diverse and their trace element distribution has been used to constrain the genetic modelling of the Proterozoic oceans and atmosphere. However, the origin of iron-formations remains controversial. They have been assigned to syn-sedimentary precipitation processes as a result of submarine exhalative, biogenic, evaporative or glacial activities (e.g. *Eugster* and *Chou*, 1973; *LaBerge*, 1973; *Fryer*, 1977; *Garrels*, 1987; *Kimberley*, 1989; *Klein* and *Beukes*, 1993). Other authors have argued for a replacement origin occurring during deformation and metamorphism (e.g. *Williams*, 1994; cf. *Davidson*, 1996), but their descriptions are commonly of epigenetic ironstones and not of iron-formations. Ironstones, in contrast to iron-formations, lack sedimentary layering, although a tectonic banding may be present. They may be controlled by pre-existing structures and rock types suitable for replacement by Fe-bearing metasomatic fluids.

Regardless of their origin, iron-formations and ironstones are guides and host rocks to metalliferous ores. Iron-formations occur in association with volcanic-

hosted and sediment-hosted massive deposits (e.g. *Stanton*, 1976; *Gustafson* and *Williams*, 1981; *Rozendaal*, 1986; *Plimer*, 1986; *Large*, 1992) and iron-formations and ironstones may host stratabound (commonly epigenetic) Au (e.g. *Phillips* et al., 1984; *Kerswill*, 1993) and Cu Au deposits (e.g. *Williams*, 1994; *Davidson* and *Large*, 1994; *Davidson*, 1994, 1996; *Adshead* et al., 1998).

Iron-formations and epigenetic ironstones are minor volume, but conspicuous rock types in the Palaeoproterozoic Willyama Supergroup of the Olary Domain, South Australia (Fig. 1) and they are also found at many locations in the adjacent Broken Hill Domain in western NSW, where some have a close spatial association with the Broken Hill PbZnAg orebodies and with CuAu mineralisation (*Stanton*, 1976; *Barnes*, 1988; *Burton*, 1994). Our work in the Olary Domain has aimed to determine the mineralogy, geochemistry and genesis of the Fe oxide-rich rocks. The present paper discusses their geological setting, field data and petrology, augmenting a previous account of the geochemistry of the Fe oxide-rich rocks and implications for mineral exploration (*Lottermoser* and *Ashley*, 1996).

## Olary Domain geology

### *Introduction*

The Olary Domain (OD) in South Australia comprises one of the inliers of the Palaeoproterozoic Willyama Supergroup in the Curnamona Province (Fig. 1). The OD is contiguous with the Broken Hill Domain (BHD) which hosts the Broken Hill PbZnAg deposit. Rocks of the OD are unconformably overlain or faulted against Neoproterozoic sedimentary rocks of the Adelaide Geosyncline. A sequence of metamorphosed clastic and chemical sediments, together with local metavolcanic and intrusive rocks is recognised in the OD, with analogies to that in the BHD (*Cook* and *Ashley*, 1992; *Flint* and *Parker*, 1993). The Willyama Supergroup is interpreted to have been deposited in an intracontinental rift setting, with subsequent intense multiphase deformation and metamorphism (*Willis* et al., 1983; *Cook* and *Ashley*, 1992; *Slack* et al., 1993). A diversity of syn-diagenetic metal enrichments occurred in the OD, some of which were related to hot spring exhalations and an evaporitic sabkha and/or playa environment. Subsequent granitic intrusive, metamorphic and deformation events have led to mobilisation of metals from the sequence and their deposition in a variety of epigenetic modes (*Bierlein* et al., 1995, 1996). The diversity of styles to metal occurrences in the OD has made it an attractive exploration location for stratiform/stratabound base metal deposits and epigenetic Cu Au and U deposits (*Ashley* et al., 1997a).

### *Olary Domain sequence*

The Willyama Supergroup in the OD may be broadly correlated with that recognised in the BHD and five lithological suits are defined (Fig. 2), which change in composition up-sequence from quartzofeldspathic-dominated to calc-silicate-bearing to pelitic (*Clarke* et al., 1986; *Stevens* et al., 1990; *Cook* and *Ashley*, 1992; *Flint* and *Parker*, 1993; *Ashley* et al., 1997a). Iron-formations occur at several different stratigraphic levels (Fig. 2).

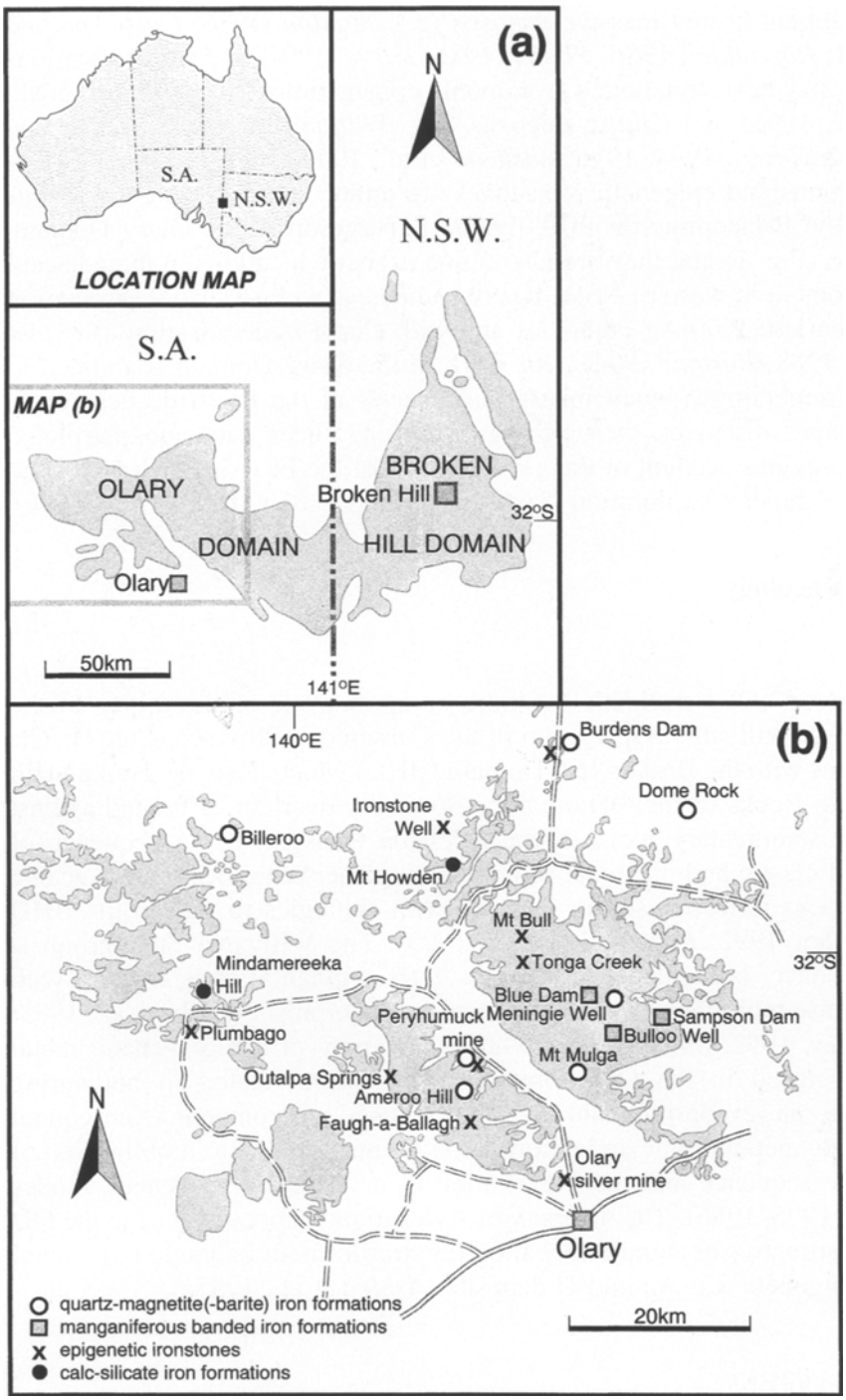


Fig. 1. **a** Location of the Olary Domain and **b** outcrop of the Willyama Supergroup showing iron-formation and ironstone occurrences (after *Lottermoser* and *Ashley*, 1996), with locations named in text

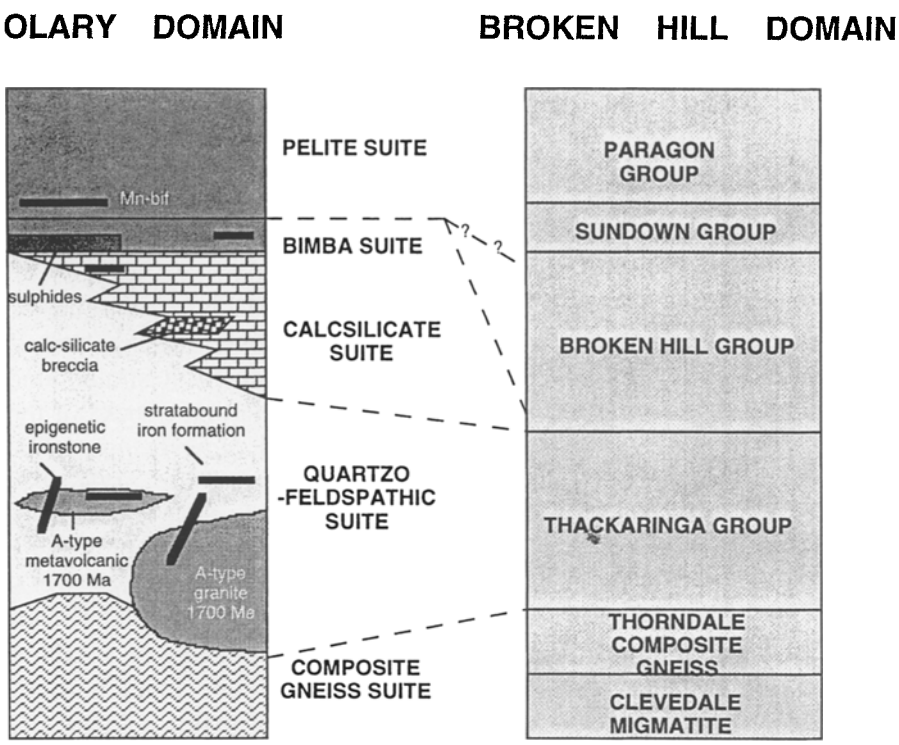


Fig. 2. Simplified stratigraphic column of the Willyama Supergroup, Olary Domain, showing major iron-formation and epigenetic ironstone occurrences (modified from *Ashley* et al., 1996)

The *Composite Gneiss Suite* (CGS) is dominated by composite gneiss and migmatite derived from quartzofeldspathic and psammopelitic rocks, as well as migmatitic leucocratic granitoids and pegmatites. The CGS is not viewed as a stratigraphic unit as its field relations imply large scale mobilisation. It grades into the *Quartzofeldspathic Suite* (QFS), which is extensively developed in the OD. The QFS is dominated by massive to layered quartzofeldspathic rocks, typically composed of sodic plagioclase + quartz, but locally with appreciable magnetite, K-feldspar and micas. There are also occurrences of psammopelitic schist and composite gneiss, quartz + Fe oxide ± barite iron-formations and reconstituted epigenetic magnetite ± hematite ± quartz ironstones. Some quartzofeldspathic gneisses in the QFS are metamorphosed A-type granitoids and rhyolitic volcanic rocks with SHRIMP U-Pb zircon ages of ~1710–1700 Ma (*Ashley* et al., 1996). The generally strongly sodic compositions in the QFS imply that felsic igneous and sedimentary precursor materials were metasomatically modified by basinal and/or metamorphic hypersaline brines (*Cook* and *Ashley*, 1992; *Ashley* et al., 1997a).

The overlying *Calcsilicate Suite* (CS) is dominated by albite + quartz + calc-silicates ± K-feldspar ± Fe oxides (calcalbitite) and minor calc-silicate-rich rocks. Calcalbitites locally contain calc-silicate pseudomorphs after former carbonate rhombs and gypsum indicating possible evaporite precursors (*Cook* and *Ashley*, 1992). Included in the CS are rare iron-formations, oxidic Mn-bearing rocks, and distinctive stratabound zones of calcsilicate matrix breccia. The latter may be

largely syn-tectonic in origin and record the passage of oxidising, hypersaline metamorphic fluids (*Yang* and *Ashley*, 1994).

The *Bimba Suite* (BS) is a thin, relatively continuous unit, conspicuous by its extensive gossanous outcrops. It displays gradational contacts with the underlying CS and QFS. The BS includes calc-silicate rocks, marble, graphitic and calc-silicate-bearing pelites and psammopelites, albite-quartz rocks and gradations into sulfide-rich rocks and rare iron-formations. Sulfide-bearing rocks contain disseminated, stratiform and vein-type Fe(CuZnPbAsCo) sulfides (*Bierlein* et al., 1995). The BS is interpreted to represent a transitional lacustrine/sabkha/marine clastic-evaporite-carbonate unit in which there were episodic hot spring exhalations. Certain sulfide-bearing calc-silicate zones in the BS may represent stratabound replacement bodies (skarn) similar to those recognised in Proterozoic rocks of the Cloncurry district in northwest Queensland (*Williams* and *Heinemann*, 1993; *Williams* and *Blake*, 1993; *Wang* and *Williams*, 1996). The *Pelite Suite* (PS) overlies the BS and is dominated by pelitic and psammopelitic schist, grading up-sequence into psammites. The lower part of the PS is commonly graphitic, with carbon isotope values indicative of a biogenic precursor (*Cook* and *Ashley*, 1992; *Bierlein* et al., 1996). There are also minor occurrences of tourmalinite, FeMn-garnet-quartz rock and manganiferous banded iron-formation (*Cook* and *Ashley*, 1992; *Ashley* et al., 1997a). The PS was deposited under more reducing conditions than other OD units and may represent a turbiditic sequence formed in a deepening marine environment.

*Structure, metamorphism and intrusive rocks*

Structural and metamorphic syntheses of the OD by *Clarke* et al. (1986, 1987) and *Flint* and *Parker* (1993) demonstrated that the Willyama Supergroup has experienced three phases of deformation ($OD_1$–$OD_3$) in the Mesoproterozoic Olarian Orogeny. Strong penetrative deformation and lower to upper amphibolite facies metamorphism occurred during $OD_1$ and $OD_2$, with the former possibly occurring prior to 1640 Ma, and the latter occurring at about $1600 \pm 20$ Ma (*Ashley* et al., 1997a). These were overprinted by retrogressive (greenschist) $OD_3$ structures at about 1500–1580 Ma. Subsequently, two further deformation events ($DD_1$–$DD_2$) occurred during the Delamerian Orogeny at about 500 Ma, attended by middle to upper greenschist facies metamorphism (*Flint* and *Parker*, 1993), and although effects are mostly manifest in the Adelaidean cover sequence rocks, they are also evident in retrograde schist zones and pegmatites cutting the Willyama Supergroup (*Lu* et al., 1996).

Several suites of granitoids and mafic intrusions are recognised in the OD. The earliest granitoid suit, emplaced at $\sim$1710–1700 Ma, predates the high grade metamorphism and deformation and has A-type chemical composition. It is genetically related to felsic metavolcanic rocks in the QFS (*Ashley* et al., 1996). Minor volumes of tholeiitic dolerite and gabbro may have been emplaced following deformation of the A-type rocks, but prior to the intrusion of a suite of mafic I-type granitoids at 1640–1630 Ma (*Ashley* et al., 1997a). A voluminous suite of leucocratic potassic to sodic S-type granitoids with an age of $1600 \pm 20$ Ma (*Cook* et al., 1994) is of regional extent in the OD and is accompanied by numerous

pegmatite bodies (*Lottermoser* and *Lu*, 1997). This suite has formed by partial melting of the WS sequence. Several occurrences of UThREE mineralisation are associated with the S-type granitoids and pegmatites (*Ashley*, 1984a; *Battey* et al., 1987; *Lottermoser* and *Lu*, 1997). Late dykes of tholeiitic dolerite were intruded at about 820 Ma, commonly into $OD_3$ structures (cf. *Wingate* et al., 1998).

### *Alteration*

Regional and local scale hydrothermal alteration was imposed on diverse rock types in the OD. Effects are structurally and lithologically-controlled and occurred during and following the Olarian Orogeny. Effects of alteration in the OD have been found in most parts of the sequence and intrusive rocks; they are most conspicuous in quartzofeldspathic compositions (albite ± Fe oxide ± biotite alteration), calc-silicate-bearing and mafic rocks (brecciation and CaFeNa silicate alteration) and iron-formations (Fe oxide ± quartz ± sulfide alteration and local brecciation). The types of alteration are thus variations on a NaFeCa metasomatic theme. Mineral compositions and fluid inclusion data imply that hydrothermal alteration throughout the OD was caused by medium to high temperature ( ~ 350°–650 °C), oxidising (generally at or above the hematite-magnetite (HM) oxygen fugacity buffer) and hypersaline (25–40 equivalent wt. % NaCl) fluids (*Kent* et al., in prep.). There is no unequivocal link between the generation of these fluids and granitoids; instead it is envisaged that episodic pulses of metamorphogenic fluid were expelled from the OD sequence (cf, *Bierlein* et al., 1995), with contributions from pre-existing evaporitic rock types (cf. *Oliver*, 1995; *Barton* and *Johnson*, 1996; *Wang* et al., 1998).

## Field occurrence and petrography of iron-formations and ironstones

### *Classification*

Iron-formations in the Olary Domain are defined as Fe-rich (>15 wt.% Fe; *Kimberley*, 1989), commonly laminated rocks, concordant with the recognised stratigraphic sequence. They are dominantly oxide and silicate facies types and are interpreted to be primary components of the stratigraphy which have undergone deformation and metamorphic recrystallisation. Samples with less than 15 wt.% Fe are more appropriately termed ferruginous quartzite. Barite-rich rocks are Ba-rich (>10 wt.% BaO) and occur in association with iron-formations. On the other hand, ironstones are defined as Fe oxide-rich epigenetic replacement bodies, generally displaying complete retexturing of pre-existing rock (generally iron-formation), with local breccia and vein textures. Field and mineralogical characteristics of the iron-formations and ironstones are summarised in Table 1 and locations of occurrences mentioned in the text are shown in Fig. 1.

### *Field occurrence*

Iron-formations hosted in the QFS are the most common Fe-rich rock in the OD, forming prominent, steeply-dipping outcrops, enclosed in laminated to massive

Table 1. *Field and mineralogical characteristics of iron-formations and ironstones in the Olary Domain*

*Quartz-Fe oxide iron-formations*

*Field data*: Restricted to Quartzofeldspathic Suite, with individual bodies up to several hundred metres long and up to tens of metres wide conformable with primary layering in enclosing quartzofeldspathic rocks. Folded and boudinaged, with primary laminations on a scale of 1 mm to several cm and intercalated with and grade into stratiform barite-rich rocks (Fig. 3A). Variable replacement and veining by epigenetic ironstones showing massive and brecciated textures or crude tectonic layering.

*Mineralogy*: Dominated by medium to coarse grained quartz and magnetite, with local variations into types with abundant hematite, albite, K-feldspar and barite. Local minor muscovite, biotite, actinolite, epidote, carbonate, biotite-phlogopite, chlorite, pyrite and chalcopyrite.

*Barite-rich rocks*

*Field data*: Restricted to Quartzofeldspathic Suite, with individual bodies up to 800 m long and 30 m wide. Intercalated with, and grade into, quartz-Fe oxide iron-formations and conformable with primary layering in enclosing quartzofeldspathic rocks. Locally folded and displaying crude laminations (scale of tens of cm to metres). Gradations into texturally reconstituted ironstones, including brecciated types.

*Mineralogy*: Dominated by coarse grained barite, quartz, magnetite (Fig. 3B) and hematite. Rare occurrence of epidote, actinolite, carbonate, biotite, pyrite, chalcopyrite, bornite.

*Calc-silicate iron-formations*

*Field data*: Up to 150 m in length and 1.5 m in thickness in Calcsilicate and Bimba Suites. Well-laminated, on a scale of 0.2 mm to several mm, with laminae conformable with primary layering in enclosing calcalbitite, calc-silicate rocks and pelite.

*Mineralogy*: Fine to medium grained albite, quartz, hematite, variable amounts of CaNaFe clinopyroxene, CaFe(Na) amphiboles, andradite and minor to trace amounts of K-feldspar, phlogopite, apatite, magnetite and titanite.

*Manganiferous iron-formations*

*Field data*: Restricted to lower part of Pelite Suite, where they are enclosed conformably as bodies up to 5 m thick and up to several tens of metres in length, within pelitic and psammopelitic schist (locally FeMn-garnet-bearing). They are well-laminated to massive (Figs. 3C, D), locally associated with thin (<1 m) conformable layers of massive to weakly laminated FeMn-garnet-quartz (-grunerite) rocks.

*Mineralogy*: Major minerals are combinations of manganoan grunerite, FeMn-garnet, quartz, magnetite and manganoan fayalite. Local minor apatite and traces of biotite, hornblende, tourmaline, epidote, ilmenite, chalcopyrite and pyrrhotite.

*Epigenetic ironstones*

*Field data*: Mostly occur as massive, veined and breccia replacements (Fig. 3E) of pre-existing quartz-Fe oxide iron-formations in the Quartzofeldspathic Suite, but have locally formed by replacement of albite-quartz-Fe oxide rocks and manganiferous iron-formation. Occur as stratabound and locally transgressive bodies up to tens of metres across and several hundred metres in length.

*Mineralogy*: Dominated by medium to coarse grained hematite, magnetite and quartz, grading into magnetite-hematite-rich. Local barite, albite and pyrite, and traces of muscovite. chalcopyrite and apatite.

albite-quartz (Fe oxide) rock. The largest outcrops (e.g. Dome Rock, Billeroo) constitute bodies up to several hundred metres long and tens of metres wide which have been folded and boudinaged. There are gradations between Fe oxide-rich, quartz-rich and barite-rich types (Figs. 3A, 3B). The latter occur at several locations in the Olary Domain (e.g. Mt Mulga, Meningie Well, Ameroo Hill) and showing lateral and vertical variations into iron-formation, ferruginous quartzite and quartzofeldspathic gneiss. Locally, laminated calc-silicate rocks occur nearby (e.g. Billeroo, Mt Bull) and south of Ameroo Hill, there is a lateral gradation into carbonate-calc-silicate rock. Two small occurrences of laminated iron-formations are known in association with calc-silicate-bearing rocks of the Calcsilicate and Bimba Suites (Mindamereeka Hill, Mt Howden area). Several occurrences of folded, laminated to massive, black Mn oxide-stained, Mn-bearing iron-formation and associated FeMn-garnet-quartz rocks are hosted within pelitic and psammopelitic schist in the Blue Dam, Bulloo Well and Sampson Dam areas (Figs. 3C, 3D). Mapping indicates that these occurrences are in the lower part of the Pelite Suite and in a psammopelite-pelite package with regional-scale Mn-enrichment, manifest by disseminated garnet.

Replacive and cross-cutting masses of epigenetic Fe oxide-rich rocks (magnetite $\pm$ hematite $\pm$ quartz ironstones) occur at several locations in the OD (Fig. 3E). At Dome Rock, Ironstone Well and Plumbago South, brecciation has occurred with coarse angular clasts of Fe oxides enclosed in a matrix of Fe oxides, quartz or barite, or of silicified albitite enclosed in Fe oxides. At several locations (e.g. Faugh-a-Ballagh, Tonga Creek, Drew Hill, Abminga Station and near Mt Bull), coarse magnetite (-quartz-hematite-pyrite) veining and breccia infill has taken place in fractured quartzofeldspathic rocks. There is no consistent spatial association between epigenetic ironstones and intrusive rocks.

Many massive Fe oxide (-quartz)-rich bodies appear to be stratabound but lack fine compositional laminations; instead they commonly exhibit a tectonic fabric with schlieren and veins of Fe oxides and quartz conformable with the foliation in adjacent rocks (e.g. Ironstone Well, Plumbago South, Burdens Dam, Mt Bull, Ameroo Hill, Outalpa Springs). These ironstones, containing recrystallised coarse grained Fe oxide-quartz assemblages, with no delicate compositional layering, are considered to be texturally reconstituted iron-formations and replacements of adjacent rocks such as laminated Fe oxide-quartz-feldspar rock (e.g. Dome Rock, Billeroo, Mt Bull). Several iron-formations displaying textural reconstitution host minor disseminated sulfide-hosted Cu and Au mineralisation, e.g. at Olary Silver mine, Mt Mulga and Peryhumuck.

*Petrography*

Iron-formations and barite-rich rocks in the Quartzofeldspathic Suite are dominated by a medium to coarse grained, granoblastic to weakly foliated assemblage, with a compositional range from magnetite-quartz to barite-rich, locally with coarse platy hematite, minor actinolite and a trace of apatite. Magnetite is partly to completely martitised as a result of supergene oxidation. Primary compositional layering is locally well-preserved. There are compositional gradations into quartzofeldspathic rock types with the incoming of albite, plus rare

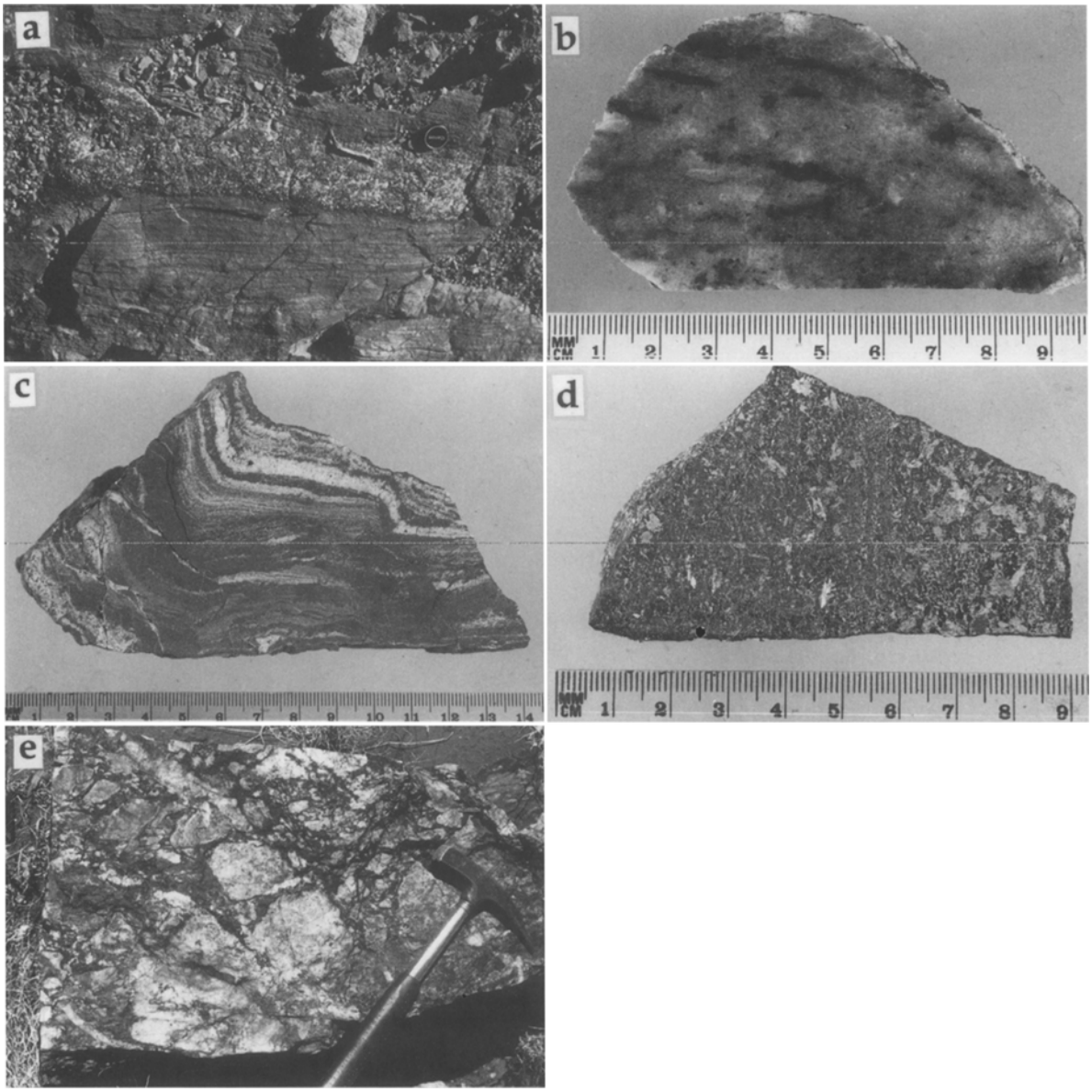


Fig. 3. **a** Well laminated quartz-magnetite iron-formation and massive barite-quartz-magnetite rock. Dome Rock, AMG (Australian Mapping Grid reference) 447000mE, 6474900mN. **b** Slab of massive barite-quartz-magnetite rock with schlieren of magnetite. Ameroo Hill, AMG 425300mE, 6443300mN. **c** Slab of finely laminated and folded manganiferous magnetite-quartz-hematite iron-formation. Blue Dam, AMG 439240mE, 6450830mN. **d** Slab of massive grunerite-fayalite-magnetite iron-formation, with coarse porphyroblastic grunerite. Bulloo Well, AMG 442680mE, 6449390mN. **e** Hematite+magnetite±quartz veins and breccia fillings in albite-quartz-albite host rock. Faugh-a-Ballagh, AMG 424620mE, 6438880mN

K-feldspar, muscovite and biotite, and into calc-silicate-bearing rocks with the presence of actinolite, epidote, carbonate, green biotite and chlorite. Minor disseminated sulfides occur at several locations (e.g. Mt. Mulga, Peryhumuck mine, Ameroo Hill South, Olary silver mine) and are dominated by pyrite and chalcopyrite, with rare bornite, pyrrhotite, cubanite and sphalerite; the sulfides may represent the effects of epigenetic overprinting. Granoblastic quartz in many iron-formations contains primary and pseudosecondary hypersaline fluid inclusions.

The small calcalbitite-hosted silicate-oxide facies iron-formation at Mindamereeka Hill is prominently laminated on a scale of 1–30 mm. Individual laminae are rich in fine to medium grained granoblastic albite + quartz, platy hematite and prismatic clinopyroxene, with amphibole and garnet being locally conspicuous in silicate-rich layers (Fig. 4A). Minor to trace amounts of K-feldspar, phlogopite, apatite, magnetite and titanite are also present. Most minerals are in textural equilibrium, although amphibole has locally replaced clinopyroxene. The iron-formation is unusual in containing yellowish-green aegirine-augite (Table 2, analysis 1) with a range from 22–48 mol.% aegirine (Fig. 5A), pale blue amphibole including winchite, actinolite and richterite compositions (Table 2, analyses 2–3; Fig. 5B) and brown andradite-rich garnet (Table 2, analysis 4; Fig. 6A). The garnet is similar in composition to garnets from calc-silicate alteration zones in the OD (Fig. 6A). Feldspars are near end-member compositions and contain abundant plates of hematite up to 40 μm across which impart a pink colour to the rocks. Clinopyroxene and quartz commonly contain hypersaline fluid inclusions, which, in similar calc-silicate rocks elsewhere in the OD, *Kent* et al. (in prep.) have shown to have pressure-corrected homogenisation temperatures of 350°–650 °C and salinities of 25–40 equivalent wt. % NaCl.

Weakly to well laminated manganiferous iron-formations display compositional layering on a scale of < 0.5 mm to 10 cm, with individual layers being rich in one or more of granoblastic magnetite (commonly martitised), quartz, garnet and fayalite, and prismatic grunerite (Figs. 4B, 4C). Apatite is a minor phase, and traces of biotite, hornblende, tourmaline, epidote, ilmenite, chalcopyrite and pyrrhotite are found in some samples. Grainsize typically ranges from 0.1–2 mm, but poikiloblastic grunerite attains several centimetres in length, commonly defining a foliation ($OS_2$) cross-cutting compositional layering. Associated rocks at Bulloo Well, Blue Dam and Sampson Dam (Fig. 1) and elsewhere in the OD include granoblastic garnet-quartz (-grunerite) assemblages. In the manganiferous iron-formations, garnet is almandine-spessartine (Table 2, analyses 5–8), but with a considerable range in Fe, Mn and Ca contents (Fig. 6A) and amphiboles include grunerite and traces of ferro-hornblende (Table 2, analyses 9–14). Grunerite compositions range from low-Mg types to those bordering cummingtonite and dannemorite (Fig. 6B). Olivines locally coexist with quartz and are manganoan fayalite in composition (Table 2, analyses 15–16), apatites are near end-member fluorapatite (Table 2, analysis 17), ilmenite is strongly manganoan (Table 2, analysis 18) and magnetite is close to stoichiometric.

Epigenetic breccia-type and vein ironstones (e.g. Faugh-a-Ballagh, Tonga Creek, Ironstone Well) and quartz-Fe oxide iron-formations with variable epigenetic reconstitution (e.g. Dome Rock, Billeroo, Ironstone Well, Mt Bull, Burdens Dam,

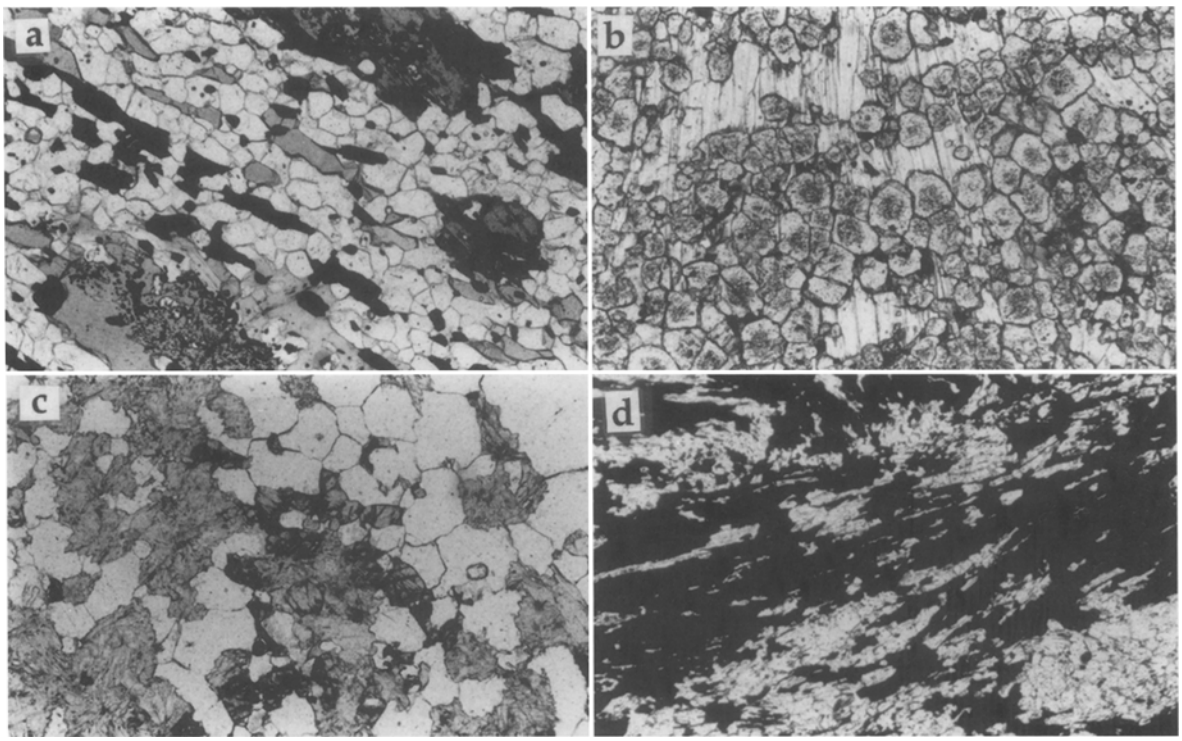


Fig. 4. **a** Foliated and weakly compositionally laminated calc-silicate iron-formation, Mindamereeka Hill, AMG 396060mE, 6453520mN, Contains platy hematite (black), clinopyroxene (dark grey, intergrown with hematite), amphibole (paler grey) and granular quartz and albite (white). Plane polarised transmitted light. Field of view 2 mm across. **b** Granular garnet intergrown with poikiloblastic grunerite in manganiferous iron-formation from Bulloo Well, AMG 442680mE, 6449390mN. Plane polarised transmitted light. Field of view 2 mm across. **c** Dark turbid grains of manganoan fayalite (centre) intergrown with quartz (clear) and grunerite (pale grey) in manganiferous iron-formation from Bulloo Well, AMG 442680mE, 6449390mN. Plane polarised transmitted light. Field of view 2 mm across. **d** Former grunerite-rich iron-formation which has been hydrothermally overprinted to form a pseudomorphous hematite (black) and quartz (white) epigenetic ironstone, Bulloo Well, AMG 442680mE, 6449390mN. Plane polarised transmitted light. Field of view 2 mm across

Peryhumuck mine, Olary silver mine) contain a simple mineral assemblage of medium to coarse grained intergrown hematite and magnetite (variably martitised) and quartz. In contrast to iron-formations in the QFS, certain retextured ironstones are composed almost entirely of massive to weakly foliated recrystallised Fe oxides, with little or no quartz. Locally, barite, albite and pyrite are present, and there are traces of muscovite, chalcopyrite and apatite. Hypersaline primary and pseudosecondary fluid inclusions are present in coarse grained quartz. Encrustations and veins of supergene Fe phosphate minerals (rockbridgeite, natrodufrenite, strengite) are present at Mt Bull and Peryhumuck mine (*Ashley* et al., 1997b). Epigenetic overprinting of a manganoan grunerite-magnetite-quartz assemblage at Bulloo Well has caused replacement by quartz-hematite (Fig. 4D).

Table 2. *Mineral chemical data for iron-formation samples from Mindamereeka Hill, Bulloo Well and Sampson Dam, Olary Domain*

| | 1 | 2 | 3 | 4 | 5 | 6 | 7 | 8 | 9 | 10 | 11 | 12 | 13 | 14 | 15 | 16 | 17 | 18 |
|---|---|---|---|---|---|---|---|---|---|---|---|---|---|---|---|---|---|---|
| $SiO_2$ | 52.03 | 55.19 | 56.36 | 35.31 | 37.05 | 36.77 | 36.03 | 35.79 | 49.05 | 47.38 | 40.53 | 50.49 | 48.26 | 50.49 | 29.03 | 28.59 | 0.18 | |
| $TiO_2$ | | | | 0.30 | | | | | | | | | | | | | | 51.43 |
| $Al_2O_3$ | 0.91 | 1.74 | 0.57 | 0.21 | 19.48 | 19.92 | 21.12 | 20.21 | | | 9.25 | 0.18 | | 0.38 | | | | 0.32 |
| $Fe_2O_3$ | 15.14 | | | 31.07 | 1.22 | 1.02 | | | | | | | | | | | | |
| FeO | 4.34 | *10.79 | *8.44 | 0.37 | 25.11 | 36.53 | *22.68 | *28.57 | *42.14 | *46.31 | *33.87 | *35.45 | *45.16 | *39.27 | *62.25 | *65.34 | *0.95 | *42.55 |
| MnO | 0.18 | | | | 13.59 | 2.84 | 17.05 | 12.07 | 4.24 | 2.77 | 0.65 | 3.76 | 2.62 | 2.63 | 8.32 | 5.69 | 0.33 | 5.82 |
| MgO | 7.61 | 17.32 | 19.39 | | | 1.18 | 0.26 | | 2.47 | 0.16 | | 7.63 | 1.62 | 4.26 | 0.41 | 0.32 | | |
| CaO | 14.19 | 7.86 | 10.30 | 32.79 | 3.55 | 1.71 | 2.80 | 3.31 | 0.12 | 0.67 | 11.32 | 0.09 | 0.09 | 0.31 | | | 54.78 | |
| $Na_2O$ | 5.64 | 3.94 | 2.09 | | | | | | | | 0.56 | | | 0.44 | | | | |
| $K_2O$ | | 0.93 | 0.59 | | | | | | | | 1.03 | | | | | | | |
| $P_2O_5$ | | | | | | | | | | | | | | | | | 40.85 | |
| F | | | | | | | | | | | | | | | | | 3.88 | |
| Cl | | | | | | | | | | | | | | | | | 0.19 | |
| $La_2O_3$ | | | | | | | | | | | | | | | | | 0.06 | |
| $Ce_2O_3$ | | | | | | | | | | | | | | | | | 0.07 | |
| $Nd_2O_3$ | | | | | | | | | | | | | | | | | 0.06 | |
| $-O=F_2$ | | | | | | | | | | | | | | | | | 1.63 | |
| $-O=Cl_2$ | | | | | | | | | | | | | | | | | 0.04 | |
| Total | 100.04 | 97.77 | 97.74 | 100.05 | 100.00 | 99.97 | 99.94 | 99.95 | 98.02 | 97.29 | 97.36 | 97.60 | 97.75 | 97.78 | 100.01 | 99.94 | 99.68 | 100.12 |

Minerals analysed by electron microprobe, with analyses in weight percent. Analysts: *J. Westaway, M.Laffan, M. Pepper and P. Ashley* at University of New England; *J. Lu* at University of Melbourne (apatite analyses). Blanks signify below detection limit. *FeO indicates total Fe as FeO. In other analyses $Fe_2O_3$ and FeO have been calculated assuming stoichiometry.

1. Clinopyroxene ($Ae_{40.4}Jd_{1.0}Q_{58.6}$), Mindamereeka Hill. Average of 26 points.
2. Winchite, Mindamereeka Hill. Average of 6 points.
3. Actinolite, Mindamereeka Hill. Average of 9 points.
4. Garnet ($Alm_{1.0}Gr_{0.1}Ad_{98.9}$), Mindamereeka Hill. Average of 7 points.
5. Garnet ($Alm_{58.6}Sp_{32.1}Gr_{5.5}Ad_{3.8}$), sample R73350, Bulloo Well. Average of 5 points.
6. Garnet ($Alm_{83.9}Sp_{6.6}Gr_{1.4}Ad_{3.3}Pyr_{4.8}$), sample R73351, Bulloo Well. Average of 6 points.
7. Garnet ($Alm_{51.6}Sp_{39.2}Gr_{8.2}Py_{1.0}$), sample BW10, Bulloo Well. Average of 5 points.
8. Garnet ($Alm_{62.3}Sp_{28.0}Gr_{4.9}Ad_{4.8}$), sample R74749, Sampson Dam. Average of 4 points.
9. Grunerite, sample R73350, Bulloo Well. Average of 6 points.
10. Grunerite, sample BW7, Bulloo Well. Average of 4 points.
11. Ferro-hornblende, sample BW7, Bulloo Well. Average of 3 points.
12. Grunerite, sample BW10, Bulloo Well. Average of 4 points.
13. Grunerite, sample BW12, Bulloo Well. Average of 5 points.
14. Grunerite, sample R74749, Sampson Dam. Average of 6 points.
15. Fayalite ($Fa_{87.2}Te_{11.8}Fo_{1.0}$), sample R73350, Bulloo Well. Average of 6 points.
16. Fayalite ($Fa_{91.2}Te_{8.0}Fo_{0.8}$), sample BW12, Bulloo Well. Average of 5 points.
17. Apatite, sample BW12, Bulloo Well. Average of 12 points.
18. Ilmenite, sample BW10, Bulloo Well. Average of 5 points.

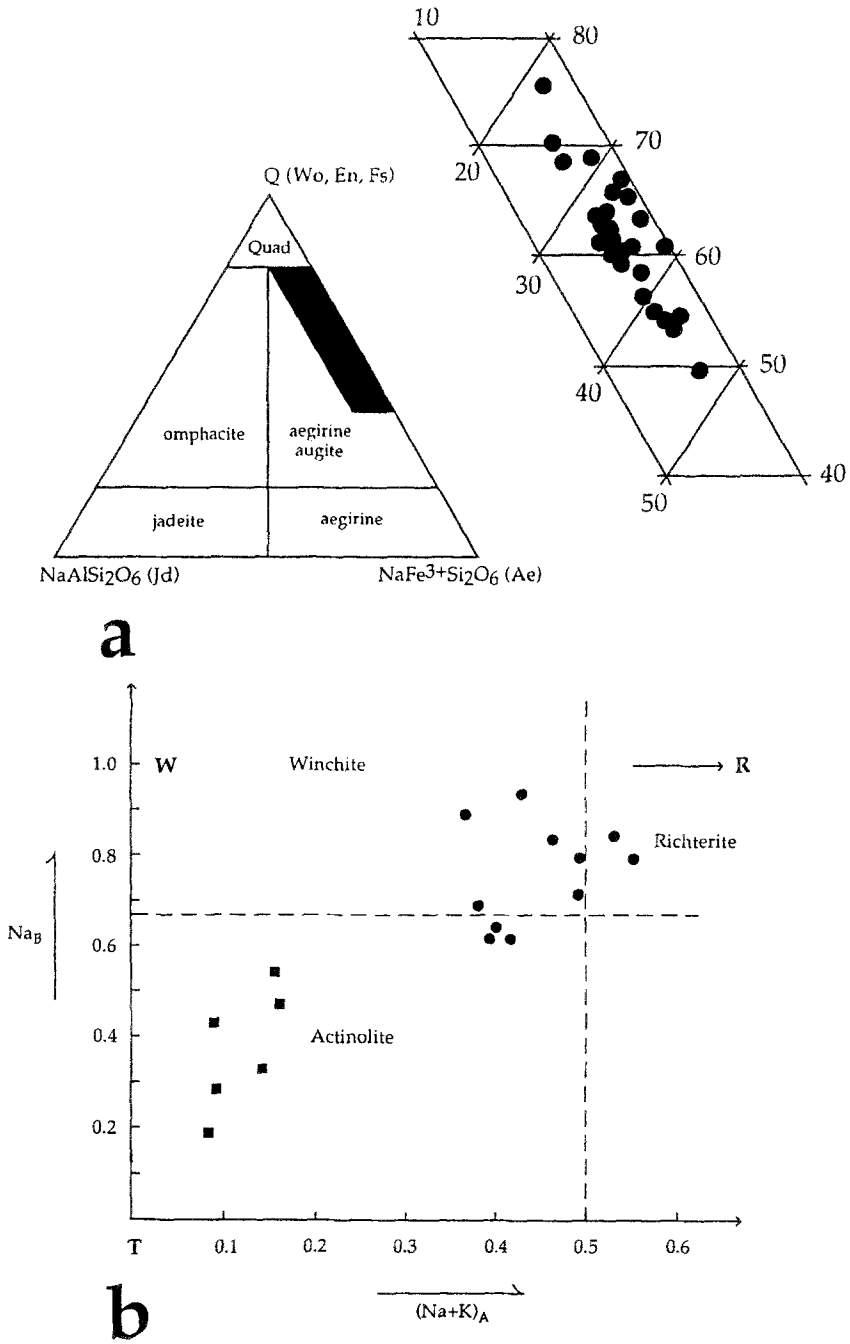


Fig. 5. **a** Plot of clinopyroxene compositions from calc-silicate iron-formation, Mindamereeka Hill, plotted in the system jadeite-aegirine-quadrilateral components (Wo, En, Fs) (after *Morimoto* et al., 1988). **b** Amphibole compositions in calc-silicate iron-formation, Mindamereeka Hill. Compositions are in the tremolite-winchite-richterite plane (from *Leake,* 1978). The origin (T = tremolite) corresponds to $Ca_2L_5Si_8O_{22}(OH)_2$, W = winchite ($CaNaL_4MSi_8O_{22}(OH)_2$) and R = richterite ($NaCaNaL_5Si_8O_{22}(OH)_2$) at $(Na+K)_A = 1.0$, $Na_B = 1.0$. L = Mg, $Fe^{2+}$, Mn. M = $Fe^{3+}$, $Al^{vi}$. Squares, sample R68564 and circles, sample R70569

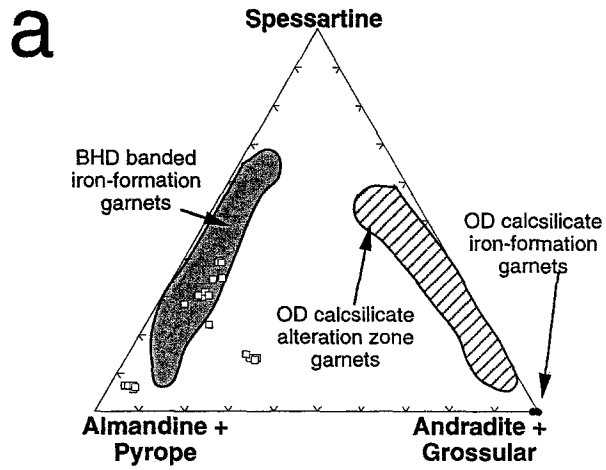


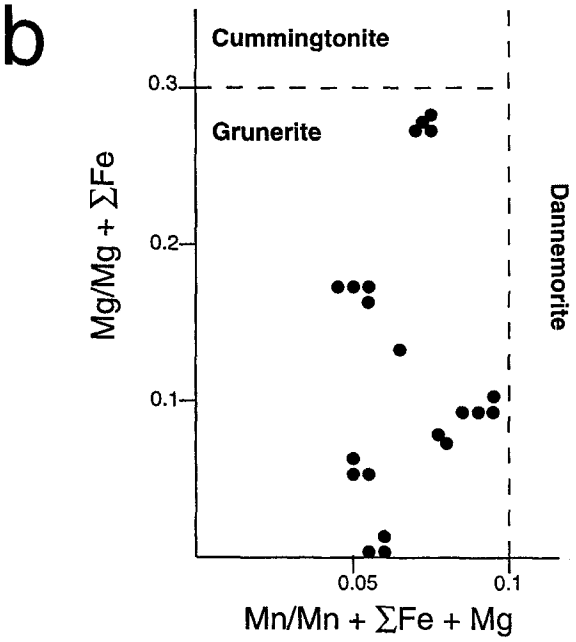


Fig. 6. **a** Compositions of garnets from OD calc-silicate iron-formations (black circles) and from manganiferous banded iron-formations (open squares) in the system spessartine – almandine + pyrope – andradite + grossular. Also shown are compositional fields of garnets from banded iron-formations in the BHD (from *Stanton*, 1976) and from calc-silicate alteration zones in the OD (*Kent* et al., in prep.). **b** Compositions of grunerite from OD manganiferous iron-formations. FeMgMn amphibole nomenclature from *Leake* (1978)

## Geochemistry

### *Methods*

Our geochemical data base contains 83 analyses of iron-formations and ironstones which were collected from surface outcrops in the Olary Domain. Samples were crushed and pulverised in a tungsten carbide ring mill. Major and minor trace elements were analysed by X-ray fluorescence spectrometry on fused discs and

pressed powder pellets at the Division of Earth Sciences, University of New England. Selected REE and Ag, As, Au, Cs, Hf, Sb, Sc, Ta, Th and U were determined by INAA at Becquerel Laboratories, Sydney. Details of the geochemistry of many iron-formations and ironstones have been reported by *Lottermoser* and *Ashley* (1996), but further data now augment the earlier study. Average compositions of the different types of iron-formations, barite-rich rocks and epigenetic ironstones are shown in Table 3A–E.

*Iron-formations and barite-rich rocks in the Quartzofeldspathic Suite*

Iron-formations are dominated by $SiO_2 + \Sigma Fe_2O_3$ (commonly >90 wt.%), with $\Sigma Fe_2O_3$ ranging up to 72 wt.%. Since individual samples may contain albite, K-feldspar, barite, epidote, actinolite and apatite, $Al_2O_3$, CaO, $Na_2O$, $K_2O$, $P_2O_5$, $SO_3$, Ba and Sr are additional minor components in the average analysis (Table 3A). Concentrations of elements indicative of a clastic input into the iron-formations (Al, Ti, Na, K, Cr, Hf, Nb, Ta, Th, Y, Zr, REE) are commonly low, but they increase with increasing feldspar content. Although values of As, Au, Cu, Pb, Zn and Mn are generally low, there are rare samples with elevated Cu (up to 140 ppm).

Barite-rich rocks show a compositional trend from containing approximately equal proportions of quartz, Fe oxides and barite to types composed largely of barite. The average composition (Table 3B) shows >50 wt % $BaO + SO_3$, with high Sr (substituting into barite), but low concentrations of elements indicative of a clastic component and of Mn and P. On the other hand, average concentrations of Cu and Au are significantly anomalous and greatly enriched relative to the iron-formations (Table 3B). Individual barite-rich samples contain up to 3030 ppm Cu and 1270 ppb Au.

The Al, Na, and Ca, transition metal (Ti, Mn, Sc, Cr), high field strength element (Nb, U, Th, Zr, Hf, Pb, REE), and large ion lithophile element values (K, Rb) of the iron-formations and barite-rich rocks are lower than average upper continental crustal abundances (cf. *Taylor* and *McLennan*, 1981). The pronounced element depletions and REE patterns have been interpreted to be a result of chemical precipitation of metalliferous sediments, with little clastic input (*Lottermoser* and *Ashley*, 1996). The origin of the locally high Cu and Au contents in the barite-rich rocks remains equivocal; they could be due to syngenetic (e.g. exhalative) deposition, or a result of epigenetic overprinting under oxidising fluid conditions.

*Calc-silicate and manganiferous iron-formations*

The dominantly silicate-rich calc-silicate iron-formations contain lower Fe and higher contents of most other major elements, transition metal and high field strength elements than the quartz-Fe oxide iron-formations (Table 3C), consistent with a greater clastic component. They are also V-enriched relative to the quartz-Fe oxide iron-formations (average $\Sigma Fe_2O_3/V = 1720$ versus 3710), but depleted in Cu and Pb. Manganiferous iron-formations in the OD are geochemically distinct in containing high Fe and Mn, but are Si-poor and have low concentrations of

Table 3A. *Average compositions of iron-formations (n: 27) in the Olary Domain (quartz + magnetite ± hematite ± barite ± albite iron-formation, QFS)*

| | Mean | Standard deviation | Minimum | Maximum |
|---|---|---|---|---|
| (wt%) | | | | |
| $SiO_2$ | 50.85 | 19.50 | 24.25 | 88.59 |
| $TiO_2$ | 0.12 | 0.15 | 0.01 | 0.63 |
| $Al_2O_3$ | 2.22 | 4.47 | 0.03 | 17.04 |
| $\Sigma Fe_2O_3$ | 42.70 | 21.87 | 7.95 | 72.91 |
| MnO | 0.04 | 0.03 | 0.01 | 0.15 |
| MgO | 0.09 | 0.14 | <0.01 | 0.62 |
| CaO | 0.34 | 1.26 | <0.01 | 6.61 |
| $Na_2O$ | 0.52 | 1.51 | <0.02 | 7.77 |
| $K_2O$ | 0.71 | 2.19 | <0.01 | 10.26 |
| $P_2O_5$ | 0.15 | 0.24 | 0.01 | 1.06 |
| $SO_3$ | 0.45 | 0.83 | 0.02 | 3.82 |
| LOI | 1.02 | 1.2 | 0.12 | 6.85 |
| Total | 99.60 | 0.66 | 97.86 | 100.59 |
| (ppm) | | | | |
| Ag | <5 | – | <5 | 6 |
| As | 4 | 7.5 | <0.5 | 34 |
| Au(ppb) | 34 | 133 | <5 | 645 |
| Ba | 6714 | 13660 | <19 | 64500 |
| Co | 35 | 44 | 0.6 | 169 |
| Cr | 24 | 20 | 11 | 85 |
| Cs | <0.5 | – | <0.5 | 1.9 |
| Cu | 42 | 27 | 14 | 140 |
| Ga | 12 | 10 | <2 | 50 |
| Hf | 0.6 | 0.9 | <0.2 | 4.8 |
| Nb | 4.8 | 6.1 | <1 | 27 |
| Ni | 14 | 13 | <4 | 47 |
| Pb | 24 | 89 | <4 | 468 |
| Rb | 21 | 45 | <1 | 207 |
| Sb | 21 | 48 | <0.1 | 185 |
| Sc | 4.2 | 5.2 | <0.1 | 18 |
| Sr | 161 | 317 | <3 | 1550 |
| Ta | <1 | – | <0.5 | 2 |
| Th | 3.1 | 5.4 | <0.2 | 20 |
| U | 2.7 | 1.8 | <2 | 10 |
| V | 115 | 80 | 6 | 246 |
| Y | 10 | 14 | <1 | 58 |
| Zn | 17 | 13 | <2 | 57 |
| Zr | 24 | 42 | <3 | 183 |
| La | 18 | 22 | <0.5 | 82 |
| Ce | 31 | 40 | <2 | 144 |
| Nd | 17 | 23 | <0.7 | 89 |
| Sm | 2.2 | 2.7 | <0.1 | 9.5 |
| Eu | 0.57 | 0.54 | 0.04 | 2 |
| Tb | 0.43 | 0.39 | <0.03 | 1 |
| Ho | 0.2 | 0.34 | <0.03 | 1.3 |
| Yb | 0.58 | 0.72 | <0.07 | 2.9 |
| Lu | 0.11 | 0.11 | 0.01 | 0.39 |

Analyses by XRF (*J. Bedford*, University of New England), except for REE, Ag, As, Au, Cs, Hf, Sb, Sc, Ta, Th and U, which were determined by INAA at Becquerel Laboratories, Sydney

Table 3B. *Average compositions of barite-rich rocks (n: 19) in the Olary Domain (barite ± quartz ± magnetite ± hematite rock, QFS*

| | Mean | Standard deviation | Minimum | Maximum |
|---|---|---|---|---|
| (wt%) | | | | |
| $SiO_2$ | 29.97 | 17.72 | 1.45 | 57.19 |
| $TiO_2$ | 0.10 | 0.07 | <0.01 | 0.21 |
| $Al_2O_3$ | 0.38 | 0.56 | 0.07 | 2.09 |
| $\Sigma Fe_2O_3$ | 14.53 | 10.83 | 3.05 | 37.39 |
| MnO | 0.06 | 0.08 | 0.01 | 0.32 |
| MgO | 0.14 | 0.34 | <0.01 | 1.18 |
| CaO | 0.15 | 0.23 | <0.01 | 0.73 |
| $Na_2O$ | 0.43 | 0.26 | 0.09 | 0.97 |
| $K_2O$ | 0.05 | 0.09 | <0.01 | 0.33 |
| $P_2O_5$ | 0.03 | 0.01 | 0.02 | 0.05 |
| $SO_3$ | 18.08 | 8.53 | 6.17 | 31.04 |
| BaO | 35.44 | 16.40 | 13.09 | 60.65 |
| LOI | 0.67 | 0.46 | 0.18 | 1.60 |
| Total | 100.04 | 0.63 | 99.02 | 101.26 |
| (ppm) | | | | |
| Ag | <5 | – | <5 | <5 |
| As | 5.1 | 9.4 | <0.5 | 38 |
| Au(ppb) | 119 | 291 | <5 | 1270 |
| Co | 2.4 | 2.3 | <0.5 | 8.1 |
| Cr | 4.8 | 3.8 | <1 | 13 |
| Cs | 15 | 42 | <0.5 | 155 |
| Cu | 491 | 930 | 32 | 3030 |
| Ga | 15 | 19 | <4 | 71 |
| Hf | 1.1 | 0.7 | 0.3 | 3.1 |
| Nb | 3.7 | 1.1 | <3 | 5 |
| Ni | 24 | 28 | <5 | 100 |
| Pb | 9.5 | 3.3 | <7 | 14 |
| Rb | 18 | 18 | <4 | 63 |
| Sb | 15 | 19 | <0.1 | 58 |
| Sc | 0.5 | 0.4 | <0.1 | 1.3 |
| Sr | 5549 | 3903 | 334 | 12000 |
| Ta | <0.5 | – | <0.5 | 2.1 |
| Th | 0.4 | 0.2 | <0.2 | 1 |
| U | <2 | – | <2 | <2 |
| V | 14 | 13 | <2 | 49 |
| Y | 17 | 15 | <4 | 56 |
| Zn | 22 | 22 | <5 | 78 |
| Zr | 20 | 26 | <3 | 90 |
| La | 4.6 | 2.4 | 1.2 | 11 |
| Ce | 5.8 | 3.9 | 0.69 | 16 |
| Nd | 2.7 | 1.6 | 0.5 | 5.2 |
| Sm | 0.48 | 0.25 | 0.11 | 0.85 |
| Eu | 0.52 | 0.18 | 0.22 | 0.90 |
| Tb | 0.40 | 0.43 | <0.03 | 0.50 |
| Ho | 0.13 | 0.11 | <0.03 | 0.50 |
| Yb | 0.42 | 0.44 | 0.07 | 1.48 |
| Lu | 0.09 | 0.08 | 0.01 | 0.16 |

Analyses by XRF (*J. Bedford*, University of New England), except for REE, Ag, As, Au, Cs, Hf, Sb, Sc, Ta, Th and U, which were determined by INAA at Becquerel Laboratories, Sydney

Table 3C. *Calc-silicate iron-formations in the Olary Domain (quartz + albite + hematite + amphibole + clinopyroxene ± andradite ± phlogopite ± K-feldspar iron-formation, CS)*

| | R70569 | R68564 | R68563 |
|---|---|---|---|
| (wt%) | | | |
| $SiO_2$ | 49.15 | 50.41 | 56.49 |
| $TiO_2$ | 0.33 | 0.40 | 0.49 |
| $Al_2O_3$ | 8.73 | 8.69 | 11.34 |
| $\Sigma Fe_2O_3$ | 26.03 | 30.37 | 17.54 |
| MnO | 0.06 | 0.04 | 0.05 |
| MgO | 2.08 | 1.24 | 1.99 |
| CaO | 5.76 | 2.24 | 4.07 |
| $Na_2O$ | 6.46 | 3.89 | 5.57 |
| $K_2O$ | 0.46 | 2.05 | 2.09 |
| $P_2O_5$ | 0.28 | 0.27 | 0.22 |
| $SO_3$ | 0.01 | <0.01 | <0.01 |
| LOI | 0.34 | 0.33 | 0.26 |
| Total | 96.69 | 99.93 | 100.11 |
| (ppm) | | | |
| As | 22 | 11 | 15 |
| Ba | 69 | 157 | 181 |
| Cr | 57 | 60 | 55 |
| Cu | 27 | 11 | 12 |
| Ga | 15 | 16 | 19 |
| Nb | 10 | 8 | 12 |
| Ni | 40 | 41 | 30 |
| Pb | 6 | 6 | 6 |
| Rb | 11 | 73 | 56 |
| Sc | 12 | 12 | 8 |
| Sr | 24 | 20 | 28 |
| Th | 15 | 13 | 11 |
| U | 4 | <3 | <3 |
| V | 157 | 150 | 123 |
| Y | 20 | 11 | 16 |
| Zn | 15 | 14 | 24 |
| Zr | 100 | 116 | 148 |
| La | 15 | 66 | <5 |
| Ce | 23 | 49 | 30 |
| Nd | 17 | 15 | 13 |

Analyses by XRF (*J. Bedford*, University of New England)

elements indicative of a clastic input. They contain higher Ca and P than the quartz-Fe oxide iron-formations (due to locally significant modal apatite) and are enriched in As, Au and Zn (Table 3D). These compositional properties are similar to Mn- and P-bearing iron-formations associated with the Broken Hill orebodies (cf. *Stanton*, 1976) and they also have links with FeMn-garnet-quartz rocks within the OD (*Lottermoser* and *Ashley*, 1996) and the BHD (*Spry* and *Wonder*, 1989).

The chemical composition of metalliferous sediments is derived from contributions from different element sources. Chemical distinctions between clastic, hydrothermal and hydrogenous components are possible using discrimina-

Table 3D. *Average compositions of manganiferous iron-formations (n: 10) in the Olary Domain (grunerite + garnet + magnetite + quartz + fayalite + apatite iron-formation, PS)*

| | Mean | Standard deviation | Minimum | Maximum |
|---|---|---|---|---|
| (wt%) | | | | |
| $SiO_2$ | 27.24 | 17.12 | 4.30 | 60.25 |
| $TiO_2$ | 0.07 | 0.06 | 0.01 | 0.21 |
| $Al_2O_3$ | 1.37 | 2.19 | <0.01 | 7.23 |
| $\Sigma Fe_2O_3$ | 66.71 | 18.13 | 36.85 | 90.70 |
| MnO | 2.90 | 2.69 | 0.04 | 7.63 |
| MgO | 0.37 | 0.35 | 0.03 | 0.97 |
| CaO | 0.68 | 0.64 | 0.10 | 1.78 |
| $Na_2O$ | 0.08 | 0.06 | <0.01 | 0.22 |
| $K_2O$ | 0.02 | 0.01 | 0.01 | 0.05 |
| $P_2O_5$ | 0.51 | 0.51 | 0.10 | 1.60 |
| $SO_3$ | 0.06 | 0.04 | 0.02 | 0.13 |
| LOI | 0.59 | 1.29 | 0.10 | 2.00 |
| Total | 99.94 | 0.44 | 99.25 | 100.70 |
| (ppm) | | | | |
| Ag | <5 | – | <5 | <5 |
| As | 48 | 74 | 3.1 | 238 |
| Au(ppb) | 19 | 20 | <5 | 60 |
| Ba | 93 | 61 | 26 | 195 |
| Co | 74 | 28 | 27 | 104 |
| Cr | 14 | 8 | <3 | 28 |
| Cs | <1 | – | <0.5 | 1.2 |
| Cu | 58 | 22 | 33 | 103 |
| Ga | 10 | 4 | 4 | 16 |
| Hf | <0.5 | – | <0.2 | 0.5 |
| Nb | 4.1 | 3.6 | <2 | 14 |
| Ni | 9.7 | 7 | <2 | 21 |
| Pb | 13 | 4 | 5 | 19 |
| Rb | 6.4 | 4 | <2 | 14 |
| Sb | <0.2 | – | <0.1 | 0.4 |
| Sc | 1.3 | 0.5 | 0.3 | 1.6 |
| Sr | 94 | 98 | 5 | 317 |
| Ta | <1 | – | <0.5 | <1 |
| Th | 2 | 2.5 | <0.5 | 8 |
| U | 16 | 7.2 | 6.5 | 30 |
| V | 139 | 85 | 6 | 297 |
| Y | 8.4 | 5.2 | <2 | 19 |
| Zn | 355 | 306 | 26 | 846 |
| Zr | 25 | 40 | 2 | 138 |
| La | 57 | 87 | 3.9 | 285 |
| Ce | 60 | 68 | 4.1 | 227 |
| Nd | 27 | 15 | 9.1 | 45 |
| Sm | 2.3 | 1.7 | 0.27 | 4.5 |
| Eu | 1 | 0.57 | <0.5 | 1.9 |
| Tb | 0.77 | 0.26 | 0.52 | <1 |
| Ho | 0.47 | 0.02 | 0.45 | 0.49 |
| Yb | 0.51 | 0.13 | 0.35 | 0.78 |
| Lu | 0.15 | 0.08 | 0.03 | <0.2 |

Analyses by XRF (*J. Bedford*, University of New England), except for REE, Ag, As, Au, Cs, Hf, Sb, Sc, Ta, Th and U, which were determined bu INAA at Becquerel Laboratories, Sydney

Table 3E. *Average compositions of epigenetic ironstones (n: 24) in the Olary Domain (magnetite + hematite + quartz ± albite ± pyrite epigenetic ironstone, QFS)*

| | Mean | Standard deviation | Minimum | Maximum |
|---|---|---|---|---|
| (wt%) | | | | |
| $SiO_2$ | 28.14 | 25.90 | 0.85 | 97.58 |
| $TiO_2$ | 0.27 | 0.37 | 0.02 | 1.75 |
| $Al_2O_3$ | 1.74 | 2.55 | 0.05 | 8.10 |
| $\Sigma Fe_2O_3$ | 65.68 | 27.76 | 1.61 | 96.86 |
| MnO | 0.06 | 0.03 | 0.01 | 0.14 |
| MgO | 0.14 | 0.30 | <0.01 | 1.23 |
| CaO | 0.17 | 0.20 | 0.01 | 0.79 |
| $Na_2O$ | 0.67 | 1.33 | 0.04 | 4.59 |
| $K_2O$ | 0.17 | 0.28 | 0.01 | 1.05 |
| $P_2O_5$ | 0.57 | 1.53 | 0.03 | 7.38 |
| $SO_3$ | 0.45 | 1.00 | 0.03 | 4.72 |
| LOI | 1.70 | 1.82 | 0.08 | 8.39 |
| Total | 99.76 | 1.67 | 93.08 | 103.65 |
| (ppm) | | | | |
| Ag | <5 | – | <5 | <5 |
| As | 4.6 | 5.7 | <0.5 | 27 |
| Au(ppb) | 51 | 135 | <5 | 560 |
| Ba | 318 | 849 | <11 | 4070 |
| Co | 45 | 35 | 1 | 116 |
| Cr | 23 | 15 | 10 | 64 |
| Cs | <0.5 | – | <0.5 | 3.3 |
| Cu | 171 | 450 | 4 | 2240 |
| Ga | 15 | 8 | 2 | 35 |
| Hf | <0.2 | – | <0.2 | 3.6 |
| Nb | 7.8 | 12 | 11 | 60 |
| Ni | 21 | 16 | <5 | 64 |
| Pb | 13 | 14 | <7 | 65 |
| Rb | 9.9 | 15 | <2 | 64 |
| Sb | 12 | 33 | <0.1 | 106 |
| Sc | 10 | 10 | 0.4 | 43 |
| Sr | 38 | 60 | <3 | 288 |
| Ta | <0.5 | – | <0.5 | 0.84 |
| Th | 4.6 | 4.8 | <0.2 | 16 |
| U | 15 | 46 | <2 | 230 |
| V | 267 | 409 | 23 | 1380 |
| Y | 68 | 126 | <3 | 554 |
| Zn | 40 | 50 | <2 | 188 |
| Zr | 27 | 35 | <2 | 132 |
| La | 26 | 31 | 0.56 | 123 |
| Ce | 44 | 49 | <4 | 159 |
| Nd | 26 | 28 | 0.92 | 86 |
| Sm | 5.6 | 6.8 | 0.20 | 27 |
| Eu | 1.5 | 2.3 | 0.09 | 10 |
| Tb | 1.4 | 2.5 | <0.04 | 10 |
| Ho | 1.9 | 3.7 | <0.04 | 15 |
| Yb | 4.1 | 8.4 | 0.06 | 33 |
| Lu | 0.6 | 1.3 | <0.01 | 5.1 |

Analyses by XRF (*J. Bedford*, University of New England), except for REE, Ag, As, Au, Cs, Hf, Sb, Sc, Ta, Th and U, which were determined by INAA at Becquerel Laboratories, Sydney

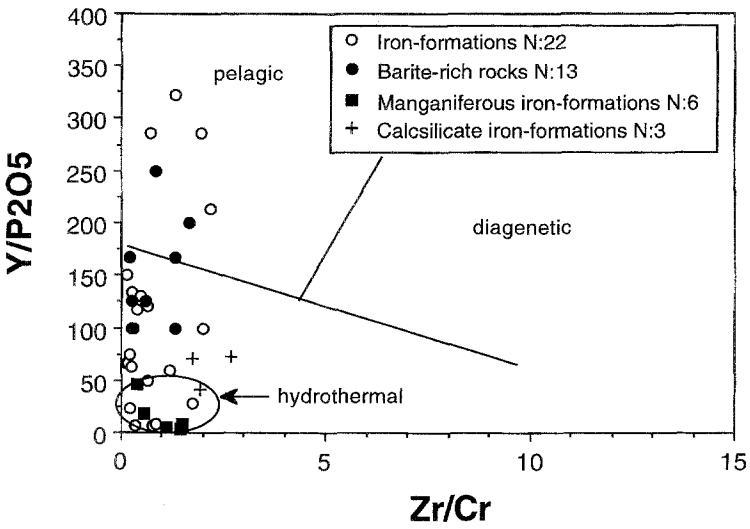


Fig. 7. $Y/P_2O_5$ versus Zr/Cr diagram for iron-formations and associated rocks of the Pelite, Calcsilicate and Quartzofeldspathic Suites (modified after *Wonder* et al., 1988)

tion diagrams (e.g. Fe/Ti versus Al/Al + Fe + Mn, *Boström*, 1973; $SiO_2$ versus $Al_2O_3$, *Wonder* et al., 1988; U versus Th, *Bonatti*, 1975; Fe-Mn-(Cu + Co + Ni)×10, *Bonatti* et al., 1972; $Y/P_2O_5$ versus Zr/Cr, *Marchig* et al., 1982; Co + Cu + Ni versus total REE, *Dymek* and *Klein*, 1988). All OD iron-formations strongly resemble hydrothermal sediments with respect to their $Y/P_2O_5$ and Zr/Cr ratios and fall either in or between the hydrothermal and pelagic sediment fields of the $Y/P_2O_5$ versus Zr/Cr diagram (Fig. 7). Data points of the OD iron-formations plot in or near the field of hydrothermal deposits of the Co + Cu + Ni versus total REE diagram (Fig. 8). All samples resemble hydrothermal sediments in that they have uniformly low Zr/Cr and Co + Cu + Ni values (Figs. 8, 9).

Thus the original chemical sediments necessary for the formation of the iron-formations in the QFS and manganiferous iron-formations were largely hydrothermal products (*Lottermoser* and *Ashley*, 1996). Contamination by clastic material (manifest in increasing contents of Al, Ti, alkalies, transition metal and high field strength trace elements) is, however, significant for a few quartz-Fe oxide and the calc-silicate iron-formations and quartz-garnet rocks as indicated, for example, by the Fe/Ti versus Al/Al + Fe + Mn discrimination diagram (*Lottermoser* and *Ashley*, 1996). Alumina-rich iron-formations are interpreted as mixed clastic and chemical sediments or as subsurface clastic sediments replaced by hydrothermal fluids.

*Epigenetic ironstones*

Compositionally, epigenetic ironstones in the QFS have similarities with the quartz-Fe oxide iron-formations, but are generally richer in Fe (up to 96–97 % $\Sigma Fe_2O_3$) and poorer in Si (Table 3E). Individual samples and the average composition of epigenetic ironstones contain higher ΣFe, Ti, P, Cu, Au, Sc, U, V, Y, Zn and heavy REE (HREE) than the iron-formations, but they contain lower Si,

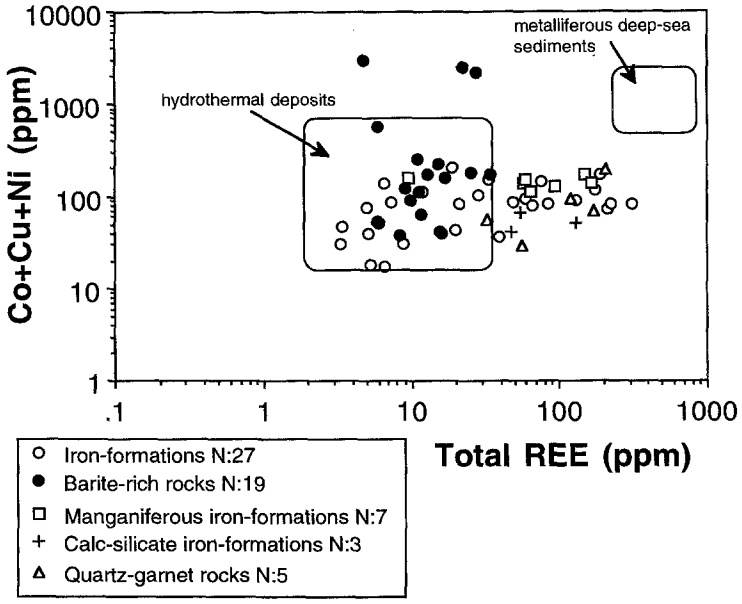


Fig. 8. (Co + Cu + Ni) versus total REE (La + Ce + Nd + Sm + Eu + Tb + Ho + Yb + Lu) diagram for iron-formations and associated rocks of the Pelite, Calcsilicate and Quartzofeldspathic Suites (modified after *Dymek* and *Klein*, 1988)

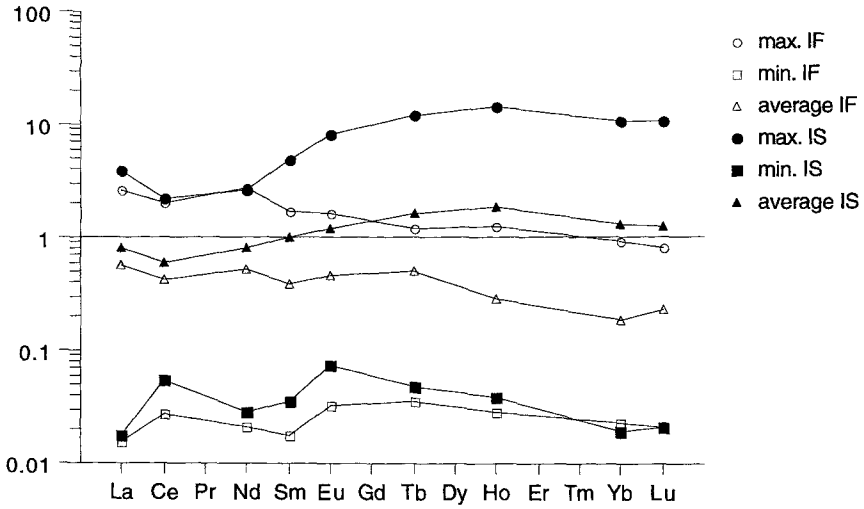


Fig. 9. NASC-normalised REE patterns for average, minimum and maximum iron-formation (IF) of the Quartzofeldspathic Suite (n: 27) and epigenetic ironstone (IS) (n: 24)

Ca, K, Ba, Rb, Sr and Pb. The epigenetic ironstones display a prominent trend to HREE-enrichment compared to the iron-formations (Fig. 9). Contents of V in the epigenetic ironstones are highly variable (up to 1380 ppm) and do not correlate well with either ΣFe or Ti. The apparent enrichment of P in the epigenetic ironstones may in part be an artifact of sampling and the inclusion of a few samples containing supergene Fe phosphate minerals (*Ashley* et al., 1997b); the actual

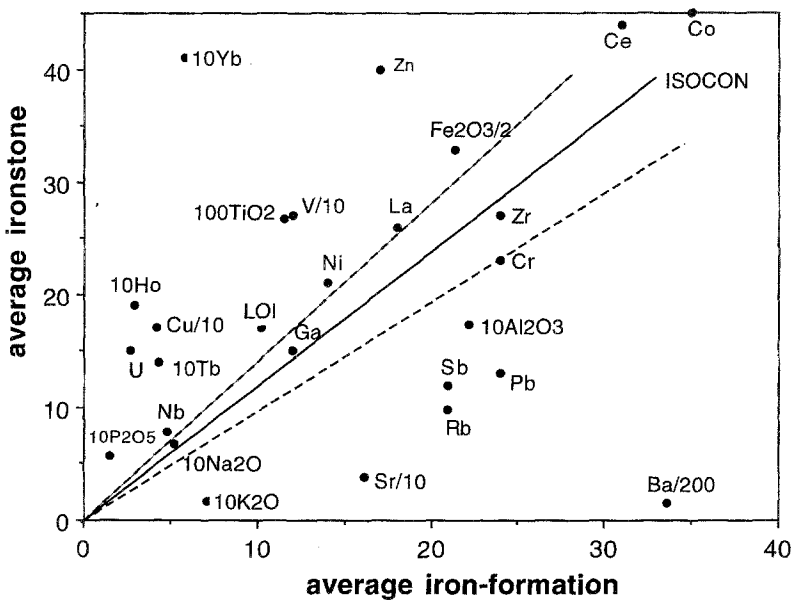


Fig. 10. Isocon diagram for average iron-formation of the Quartzofeldspathic Suite (n: 27) and average epigenetic ironstone (n: 24) using Zr and Ga as the basis for the isocon fit. Error limits calculated from the standard deviation (5%) of elements on which the isocon is based are shown by the cone around the isocon. Selected major element oxides plotted in wt%, minor elements in ppm. In reading the diagram, components above the isocon have been added, and those below subtracted

contents of primary apatite in both the epigenetic ironstones and quartz-Fe oxide iron-formations are similarly small.

The isocon approach of *Grant* (1986) to determine element mobility has been applied to the average iron-formation and epigenetic ironstone and to partly altered and magnetite-hematite veined and brecciated quartz-albite hostrocks and massive epigenetic ironstones at Mt Bull and Faugh-a-Ballagh. Comparison of the compositions of the average iron-formation with the average ironstone indicates that Fe, Ti, P, Cu, Au, Sc, U, V, Y, Zn and HREE were generally enriched (Table 3A, 3E; Fig. 10). Elements generally depleted include Si, Al, K, Ca, Ba, Rb, Sb, Sr and Pb, whereas Mg, Na, Co, Cr, Ga, Hf, Nb, Th and Zr remained largely immobile. Individual locations show highly variable element enrichments or depletions (Faugh-a-Ballagh: gain of K, Ga, Ni, Nb, S, Sc; loss of Ba; Mt Bull: gain of U, Pb, Ba, As, Ga, Th; loss of K, S, Sr, Rb). Such contrasting element behaviour suggests very localized redistribution of element during replacement.

## Discussion

### *Comparison with iron-formations and ironstones in the Broken Hill Domain and Mt Isa Eastern Succession*

Iron-formations in the QFS in the OD have stratigraphic and compositional affinities with quartz-magnetite bodies in the Thackaringa Group of the BHD

(*Willis* et al., 1983; *Burton,* 1994), and although the latter are not known to be baritic or associated with calc-silicates or Mn-rich rocks, they are locally pyritic and contain epigenetic CuAu mineralisation (*Willis* et al., 1983; *Burton*, 1994). The manganiferous iron-formations in the Pelite Suite exhibit mineralogical, compositional and stratigraphic affinities to the laminated manganiferous banded iron-formations and FeMn-garnet-quartz rocks in the upper part of the Broken Hill Group in the BHD (*Stanton*, 1976; *Barnes*, 1988; *Spry* and *Wonder*, 1989; *Lottermoser*, 1989). In the latter unit, such rocks have a spatial and possible genetic relationship to the Broken Hill PbZnAg orebodies (*Stanton*, 1976; *Plimer*, 1984; *Barnes*, 1988; *Spry* and *Wonder*, 1989). The OD manganiferous iron-formations are not as consistently phosphatic as those in the BHD, nor are they as anomalous in base metals (cf. *Stanton*, 1976); no direct association of the latter with base metal sulfide mineralisation is currently known, although at this general stratigraphic level in the Pelite Suite, disseminated ZnFe(Pb) sulfides have been found. There does not appear to be an analogue in the BHD of the calc-silicate iron-formation at Mindamereeka Hill (Fig. 1). The unusual alkali- and $Fe^{3+}$-rich rocks (Table 3C) with hematite, CaFe(Na) amphibole(s), CaNaFe clinopyroxene and andradite, could be the result of the high-temperature replacement of pre-existing laminated iron-formation (e.g. magnetite-bearing) by $NaCaFe^{3+}$ rich fluids (cf. *Williams*, 1994; *Barton* and *Johnson*, 1996; *Davidson*, 1996). Alternatively, they may have formed by the metamorphism of an extremely oxidised, mixed chemical-clastic precursor with Fe-enrichment from exhalative hot spring sources. Aegirine-bearing iron-formations are also known (e.g. *Klein*, 1966; *McSwiggen* et al., 1994) and have been interpreted to reflect the presence of Na-rich fluids during pre-, syn- and post-depositional stages (*McSwiggen* et al., 1994).

There are strong analogies between the field, mineralogical and chemical characteristics of the OD iron-formations and ironstones, and those reported from the Proterozoic Mt Isa Eastern Succession (e.g. *Davidson* et al., 1989; *Davidson*, 1996; *Adshead* et al., 1998). In the latter region, *Davidson* (1996) has proposed that there remain suites of primary iron-formations which largely retain their original chemistry (and to some extent preserve primary sedimentary features), but that in places, the iron-formations have been metasomatised and that there are also structurally- and lithologically-controlled replacement ironstones. Where there has been metasomatism, or formation of replacement ironstones, the $\Sigma Fe$ contents have increased and may be accompained by CuAu mineralisation.

### *Genesis of iron-formations and barite-rich rocks and their subsequent metamorphism*

Field data, petrology and major and trace element geochemistry indicate that the QFS iron-formations and barite-rich rocks, and the PS manganiferous iron-formations precipitated from hydrothermal fluids (*Lottermoser* and *Ashley*, 1996). Metalliferous chemical sedimentation process were operating throughout deposition of the Willyama Supergroup in the OD and formed diverse metalliferous rock types including barite-, scheelite-, tourmaline-, iron oxide-, iron sulfide-, (*Bierlein* et al., 1995), and piemontite-rich rocks (*Ashley*, 1984b). Much of this chemical

sedimentation could have occurred from hot springs exhaling into a shallow water, possibly evaporative setting in an intracontinental rift environment (*Cook* and *Ashley*, 1992), and indeed, B isotopic compositions of tourmaline-rich rocks from the adjacent BHD (*Slack* et al., 1993) are consistent with derivation from a non-marine evaporite source. Iron, Ba, Mn and other metals could have been leached from the volcano-sedimentary fill of the rift sequence by circulating heated saline fluids. Metalliferous chemical sediments are characteristic of many Proterozoic rift-type terrains and are associated with, or have potential for, massive sulfide deposits (cf. *Rozendaal*, 1986; *Plimer*, 1986; *Sawkins*, 1990).

Iron-formations in the QFS contain a medium to coarse grained recrystallised mineral assemblage of magnetite and/or hematite + quartz ± feldspars ± barite, from which little can be ascertained regarding formation conditions apart from the fact that the rocks have recrystallised at or near the HM buffer. Iron-formations transitional into calc-silicate rocks, including the small iron-formations at Mindamereeka Hill, contain assemblages with CaFe(Na) amphibole(s) ± CaNaFe clinopyroxene ± andradite, with hematite ± magnetite. Apart from being generally indicative of medium grade metamorphic conditions, it can again be inferred that $fO_2$ conditions were maintained at or above the HM buffer. Metamorphic fluids in equilibrium with quartz and clinopyroxene were hypersaline and oxidising (fluid inclusions commonly contain daughter salts and hematite, and have corrected homogenisation temperature of $\sim 350°–650°$ C; *Kent* et al., in prep.).

In the manganiferous iron-formations, the assemblage grunerite-fayalite-magnetite-garnet (almandine-spessartine) is consistent with metamorphic grade being at least staurolite-kyanite zone and possibly sillimanite zone (*Klein*, 1982) with $fO_2$ conditions approximating the quartz-fayalite-magnetite buffer. In the Bulloo Well region (Fig. 1), this accords with fibrolitic sillimanite being present in adjacent metapelite assemblages (*Laffan*, 1994) and manganiferous iron-formation contains coexistng garnet ($X_{Mn} = 0.39$, $X_{Fe} = 0.52$, $X_{Ca} = 0.08$) and ilmenite ($X_{Mn} = 0.12$) which yield a temperature estimate of 610 °C using the garnet-ilmenite geothermometer of *Pownceby* et al. (1991).

### *Genesis of epigenetic ironstones*

Recrystallisation, vein and breccia textures within the epigenetic ironstones are indicative of fluid-rock reactions. Hypersaline fluid inclusions containing solid phases including halite, anhydrite and hematite occur in quartz in epigenetic ironstones and in recrystallised quartz and clinopyroxene in the calc-silicate iron-formations. The same types of fluid inclusions are widespread throughout the OD metamorphic sequence and are characteristic of calc-silicate-rich skarn-like replacement assemblages (garnet ± quartz ± epidote), calc-silicate matrix breccias and certain albite-quartz rocks. They have been interpreted to reflect the passage of high-temperature ($\sim 350°–650$ °C), hypersaline, oxidising fluids through portions of the sequence (*Yang* and *Ashley*, 1994; *Kent* et al., in prep).

Experimental data indicate that Fe has considerable solubility in high temperature, saline hydrothermal fluids, with pressure, pH, $fO_2$ and $fS_2$ also exerting some control (e.g. *Chou* and *Eugster*, 1977; *Hemley* et al., 1992; *McPhail*, 1993). Similarly, Cu, Au, U and REE are also increasingly soluble in high

temperature, oxidising, saline fluids (e.g. *Davidson* and *Large,* 1994; *Barton* and *Johnson,* 1996).

For the OD, it is proposed that Fe was leached from the evaporite-bearing volcanosedimentary sequence by hot, saline metamorphic fluids. Iron-bearing minerals such as biotite, magnetite and hematite reacted with the fluid and the mobilised Fe was subsequently reprecipitated in suitable structural and reactive lithological sites, largely facilitated by temperature decrease and wallrock reactions (cf. *McPhail,* 1993; *Barton* and *Johnson,* 1996). Interaction of these fluids with iron-formations and Fe oxide-bearing quartzofeldspathic rocks led to strong recrystallisation, local veining, brecciation and the deposition of Fe as Fe oxides, Fe-bearing calc-silicate minerals, and to lesser degree as sulfides. The solubility of Zn and Pb remained high at temperatures greater than 300 °C in these saline fluids (with high Cl/S and low reduced S) (cf. *Hemley* et al., 1992); however, only the less soluble Cu precipitated as sulfide, with Au in elemental form or held cryptically in sulfides. Fluids responsible for epigenetic veining and brecciation were rich in $Fe^{3+}$ and caused modest enrichment in Ti, Cu, Au, Sc, U, V, Y, Zn and HREE and thus exhibit chemical characteristics of fluids responsible for the formation of syn-metamorphic ironstones in the Mt Isa Eastern Succession (cf. *Williams,* 1994). This model has direct analogies with those proposed for regional-scale alteration, Fe mobility and metasomatism in the Mt Isa Eastern Succession (e.g. *Williams,* 1994; *Williams* and *Blake,* 1993; *Davidson,* 1994; 1996; *Oliver,* 1995; *DeJong* and *Williams,* 1995) and with the evaporite source model of *Barton* and *Johnson* (1996) for epigenetic FeCuAuUREE mineralization.

The timing of alteration and brecciation in the OD was possibly episodic, and may include syn-diagenetic (cf. *Plimer,* 1977; *Cook* and *Ashley,* 1992), as well as syn-metamorphic and syn-deformational ($OD_1$–$OD_3$) events (*Yang* and *Ashley,* 1994; *Ashley* et al., 1997a). Field and Sm-Nd isotopic data constrain certain skarn-like calc-silicate replacement bodies to syn- to post-$OD_2$ at ~ 1580–1530 Ma (*Kent* et al., in prep). It is likely that ironstone genesis in the OD is simply a variation in theme of regional-scale metasomatic alteration. It is a manifestation of an ultimately evaporite-derived, saline, high-temperature and oxidised NaFeCa-bearing metamorphic fluid, imposed on an Fe-rich precursor rock type.

## Conclusions

Iron-formations of the Palaeoproterozoic Willyama Supergroup are found in three distinct geological settings. Iron-formations of the Quartzofeldspathic Suite occur in albite-quartz (-Fe oxide) rocks and consist of magnetite and quartz and minor hematite, barite, actinolite and apatite. They also show internal gradations from Fe oxide-dominant types, through examples rich in quartz, to types rich in barite. Calc-silicate iron-formations of the Calcsilicate or Bimba Suites are enclosed by calcalbitite and calc-silicate rocks. They are hematite-rich with associated magnetite, albite, quartz, CaFe(Na) amphibole(s), CaNaFe clinopyroxene and andraditic garnet. Manganiferous iron-formations of the Pelite Suite are hosted within pelitic and psammopelitic rocks and have associated garnet-quartz rock occurrences. These iron-formations comprise magnetite, quartz, almandine-spessartine, manganoan fayalite and manganoan grunerite and display mineralogical

gradations from magnetite-dominant types, through examples rich in fayalite and grunerite, to types with abundant garnet and quartz. The diverse iron-formation types are the result of metalliferous chemical sedimentation processes operating throughout the deposition of the Willyama Supergroup.

The iron-formations have experienced localised epigenetic overprints causing textural and compositional reconstitution. Epigenetic ironstones contain a simple mineral assemblage of magnetite, hematite and quartz. They are the result of the passage of syn-metamorphic, high-temperature ($\sim 350°$–$650\,°C$), saline, oxidising fluids through portion of the Willyama Supergroup sequence. Interaction of these fluid with iron-formations and Fe oxide-bearing quartzofeldspathic rocks has led to strong recrystallisation, local veining and brecciation, and the formation of epigenetic ironstones with variable Fe, Ti, Cu, Au, Sc, U, V, Y, Zn and HREE enrichment. The generation of the ironstones is viewed as part of the spectrum of regional-scale hydrothermal alteration effects, widespread in the OD.

**Acknowledgements**

The Australian Research Council, Mines and Energy South Australia, AGSO and a consortium of Australian mineral exploration companies provided funding for this study as part of the collaborative Olary Mapping Project. *M. L. Laffan, J. Lu* and *M. A. Pepper* helped with sampling, sample preparation and data acquisition and we have had useful discussions with *A. J. R. Kent* and *I. R. Plimer.* Critical comments of two Mineralogy and Petrology reviewers have further improved the manuscript.

**References**

*Adshead ND, Voulgaris P, Muscio VN* (1998) Osborne copper-gold deposit. In: *Berkman DA, Mackenzie DH* (eds) Geology of Australian and Papua New Guinean mineral deposits. Aust Inst Min Metal Monogr 22: 793–800

*Ashley PM* (1984a) Sodic granitoids and felsic gneisses associated with uranium-thorium mineralisation, Crockers Well, South Australia. Mineral Deposita 19: 7–18

*Ashley PM* (1984b) Piemontite-bearing rocks from the Olary district, South Australia. Aust J Earth Sci 31: 203–216

*Ashley PM, Cook NDJ, Fanning CM* (1996) Geochemistry and age of metamorphosed felsic igneous rocks with A-type affinities in the Willyama Supergroup, Olary Block, South Australia, and implications for mineral exploration. Lithos 38: 167–184

*Ashley PM, Lawie DC, Conor CHH, Plimer IR* (1997a) Geology of the Olary Domain, Curnamona Province, South Australia and field guide to 1997 excursion stops. Dept Mines Energy S Aust, Report Book 97/17, 51 pp

*Ashley PM, Lottermoser BG, Scott KM* (1997b) Supergene iron phosphate minerals in Proterozoic ironstones from the Olary Block, South Australia. N Jb Miner Mh 7: 309–327

*Barnes RG* (1988) Metallogenic studies of the Broken Hill and Euriowie Blocks, New South Wales. 1. Styles of mineralization in the Broken Hill Block. 2. Mineral deposits of the southwestern Broken Hill Block. Geol Surv NSW Bull 32 (1,2): 250 pp

*Barton MD, Johnson DA* (1996) Evaporitic-source model for igneous-related Fe oxide-(REE-Cu-Au-U) mineralization. Geology 24: 259–262

*Battey GC, Miezitis Y, McKay AD* (1987) Australian uranium resources. Bureau Min Res Geol Geophys Rep 1: 69 pp

*Bierlein FP, Ashley PM, Plimer IR* (1995) Sulphide mineralisation in the Olary Block, South Australia. Mineral Deposita 30: 424–438

*Bierlein FP, Ashley PM, Seccombe PK* (1996) Origin of hydrothermal Cu-Zn-Pb mineralisation in the Olary Block, South Australia: evidence from fluid inclusions and sulphur isotopes. Precamb Res 79: 281–305

*Bonatti E* (1975) Metallogenesis at ocean spreading centers. Ann Rev Earth Planet Sci 3: 401–431

*Bonatti E, Kraemer T, Rydell H* (1972) Classification and genesis of submarine iron manganese deposits. In: *Horn D* (ed) Ferromanganese deposits on the ocean floor. Nat Sci Found: 149–165

*Boström K* (1973) The origin and fate of ferromanganoan active ridge sediments. Stockholm Contrib Geol 27: 149–243

*Burton GR* (1994) Metallogenic studies of the Broken Hill and Euriowie Blocks, New South Wales. 3. Mineral deposits of the southeastern Broken Hill Block. Geol Surv NSW Bull 32(3): 100 pp

*Chou I-M, Eugster HP* (1977) Solubility of magnetite in super-critical chloride solutions. Am J Sci 277: 1296–1314

*Clarke GW, Burg JP, Wilson CJL* (1986) Stratigraphic and structural constraints of the Proterozoic tectonic history of the Olary Block, South Australia. Precamb Res 34: 107–137

*Clarke GL, Guiraud R, Powell R, Burg JP* (1987) Metamorphism in the Olary Block, South Australia: compression with cooling in a Proterozoic fold belt. J Met Geol 5: 291–306

*Cook NDJ, Ashley PM* (1992) Meta-evaporite sequence, exhalative chemical sediments and associated rocks in the Proterozoic Willyama Supergroup, South Australia: implications for metallogenesis. Precamb Res 56: 211–226

*Davidson GJ* (1994) Hostrocks to the stratabound iron-formation-hosted Starra gold-copper deposit, Australia. I. Sodic lithologies. Mineral Deposita 29: 237–249

*Davidson GJ* (1996) Styles and timing of iron enrichment in the Mt Isa Eastern Succession. In: *Baker T, Rotherham JF, Richmond JM, Mark G, Williams PJ* (eds) New developments in metallogenic research: the McArthur-Mount Isa-Cloncurry minerals province. EGRU Contribution 55: 40–43

*Davidson GJ, Large RR* (1994) Gold metallogeny and the copper-gold association of the Australian Proterozoic. Mineral Deposita 29: 208–223

*Davidson GJ, Large RR, Kary G, Osborne R* (1989) The deformed iron formation-hosted Starra and Trough tank Au-Cu mineralization: a new association from the Proterozoic Eastern Succession of Mt Isa, Australia. In: *Keays RR, Ramsay WRH, Groves DI* (eds) The geology of gold deposits: the perspective in 1988. Econ Goel Monogr 8: 135–150

*De Jong G, Williams PJ* (1995) Giant metasomatic system formed during exhumation of mid-crustal Proterozoic rocks in the vicinity of the Cloncurry Fault, northwest Queensland. Aust J Earth Sci 42: 281–290

*Dymek RF, Klein C* (1988) Chemistry, petrology and origin of banded iron-formation lithologies from the 3800 Ma Isua Supracrustal Belt, West Greenland. Precamb Res 39: 247–302

*Eugster HP, Chou I-M* (1973) The depositional environments of precambrian banded iron-formations. Econ Geol 68: 1144–1168

*Flint RB, Parker AJ* (1993) Willyama Inliers. In: *Drexel JF, Preiss WV, Parker AJ* (eds) The geology of South Australia, vol 1. The Precambrian. Geol Surv South Aust Bull 54: 82–93

*Fryer BJ* (1977) Trace element geochemistry of the Sokoman Iron Formation. Can J Earth Sci 14: 1598–1610

*Garrels RM* (1987) A model for the deposition of the microbanded Precambrian iron formations. Am J Sci 287: 81–106

*Grant JA* (1986) The isocon diagram – a simple solution to Gresens' equation for metasomatic alteration. Econ Geol 81: 1976–1982

*Gustafson LB, Williams N* (1981) Sediment-hosted stratiform deposits of copper, lead and zinc. In: *Skinner BJ* (ed) Econ Geol 75th Anniversary Volume: 139–178

*Hemley JJ, Cygan GL, Fein JB, Robinson GR, D'Angelo WM* (1992) Hydrothermal ore-forming processes in the light of studies in rock-buffered systems. I. Iron-copper-zinc-lead-sulfide solubility relations. Econ Geol 87: 1–22

*Kent AJR, Ashley PM, Fanning CM* (1998) Metasomatic garnet-epidote alteration zones in the Willyama Supergroup, Olary Domain, South Australia (in preparation)

*Kerswill JA* (1993) Models for iron-formation-hosted gold deposits. In: *Kirkham RV, Sinclair WD, Thorpe RI, Duke JM* (eds) Mineral deposit modeling. Geol Assoc Canada, Spec Pap 40: 171–199

*Kimberley MA* (1989) Nomenclature for iron-formations. Ore Geol Rev 5: 1–12

*Klein C* (1966) Mineralogy and petrology of the metamorphosed Wabush Iron Formation, southwestern Labrador. J Petrol 7: 246–305

*Klein C* (1982) Amphiboles in iron-formations. In: *Veblen DR, Ribbe PH* (eds) Amphiboles: petrology and experimental phase relations. Min Soc Am, Washington, pp 88–98 (Rev Mineral 9B)

*Klein C, Beukes NJ* (1993) Sedimentology and geochemistry of the glaciogenic Rapitan iron-formation in Canada. Econ Geol 88: 542–565

*La Berge GL* (1973) Possible biological origin of Precambrian iron-formations. Econ Geol 68: 1098–1109

*Laffan ML* (1994) Geology and magnetic studies in the Meningie Well-Blue Dam area, Olary Domain, South Australia. Thesis, University of New England (unpublished)

*Large RR* (1992) Australian volcanic-hosted massive sulfide deposits: feature, styles, and genetic models. Econ Geol 87: 471–510

*Leake BE* (1978) Nomenclature of amphiboles. Am Mineral 63: 1023–1052

*Lottermoser BG* (1989) Rare earth element study of exhalites within the Willyama Supergroup, Broken Hill Block, Australia. Mineral Deposita 24: 92–99

*Lottermoser BG, Ashley PM* (1996) Geochemistry and exploration significance of ironstones and barite-rich rocks in the Proterozoic Willyama Supergroup, Olary Block, South Australia. J Geochem Explor 57: 57–73

*Lottermoser BG, Lu J* (1997) Petrogenesis of rare-element pegmatites in the Olary Block, South Australia, part 1. Mineralogy and chemical evolution. Mineral Petrol 59: 1–19

*Lu J, Plimer IR, Foster DA, Lottermoser BG* (1996) Multiple post-orogenic reactivation in the Olary Block, South Australia: evidence from $^{40}Ar/^{39}Ar$ dating of pegmatitic muscovite. Int Geol Rev 38: 665–685

*Marchig V, Gundlach H, Möller P, Schley F* (1982) Some geochemical indicators for discrimination between diagenetic and hydrothermal metalliferous sediments. Mar Geol 50: 241–256

*McPhail DC* (1993) The behaviour of iron in high-temperature chloride brines. Geol Soc Aust Abstr 34: 50–51

*McSwiggen PL, Morey GB, Cleland JM* (1994) The origin of aegirine in iron-formation of the Cuyuna Range east-central Minnesota. Can Mineral 32: 589–598

*Morimoto N, Fabries J, Ferguson AK, Ginzburg IV, Ross M, Siefert FA, Zussman J* (1988) Nomenclature of pyroxenes. Am Mineral 73: 1123–1133

*Oliver NHS* (1995) Hydrothermal history of the Mary Kathleen Fold Belt, Mt Isa Block, Queensland. Aust J Earth Sci 42: 267–279

*Phillips GN, Groves DI, Martyn JE* (1984) An epigenetic origin for Archean banded iron-formation hosted gold deposits. Econ Geol 79: 162–171

*Plimer IR* (1977) The origin of albite-rich rocks enclosing the cobaltian pyrite deposit at Thackaringa, NSW, Australia. Mineral Deposita 12: 175–187

*Plimer IR* (1984) The mineralogical history of the Broken Hill Lode, NSW. Aust J Earth Sci 31: 379–402

*Plimer IR* (1986) Sediment-hosted exhalative Pb-Zn deposits – products of contrasting ensialic rifting. Trans Geol Soc South Africa 89: 57–73

*Pownceby MI, Wall VJ, O'Neill H St C* (1991) An experimental study of the effect of Ca upon garnet-ilmenite Fe-Mn exchange equilibria. Am Mineral 76: 1580–1588

*Rozendaal A* (1986) The Gamsberg zinc deposit, Namaqualand district. In: *Anhaeusser CR, Maske S* (eds) Mineral deposits of southern Africa. Geol Soc S Afr, Johannesburg, pp 1477–1488

*Sawkins FJ* (1990) Metal deposits in relation to plate tectonics. Springer, Berlin Heidelberg New York Tokyo

*Slack JF, Palmer MR, Stevens BPJ, Barnes RG* (1993) Origin and significance of tourmaline-rich rocks in the Broken Hill district, Australia. Econ Geol 88: 505–541

*Spry PG, Wonder JD* (1989) Manganese-rich garnet rocks associated with the Broken Hill lead-zinc-silver deposit, New South Wales, Australia. Can Mineral 27: 275–292

*Stanton RL* (1976) Petrochemical studies of the ore environment at Broken Hill, New South Wales: 1 – constitution of 'banded iron-formation'. Trans Inst Min Metall Sect B 85: B33–B46

*Stevens BPJ, Barnes RG, Forbes BG* (1990) Willyama Block – regional geology and minor mineralisation. In: *Hughes FE* (ed) Geology of the mineral deposits of Australia and Papua New Guinea. Aust Inst Min Metall Monogr 14: 1065–1072

*Taylor SR, McLennan SM* (1981) The composition and evolution of the continental crust: rare earth element evidence from sedimentary rocks. Phil Trans R Soc A301: 381–399

*Wang A-J, Peng Q-M, Palmer MR* (1998) Salt dome-controlled sulfide precipitation of Paleoproterozoic Fe-Cu sulfide deposits, eastern Liaoning, northeastern China. Econ Geol 93: 1–14

*Wang S, Williams PJ* (1996) Alteration and mineralization styles of the skarn-hosted Mount Elliott Cu-Au deposit and adjacent SWAN prospect, Cloncurry district. In: *Baker T, Rotherham JF, Richmond JM, Mark G, Williams PJ* (eds) New developments in metallogenic research: the McArthur-Mount Isa-Cloncurry minerals province. EGRU Contribution 55: 139–142

*Williams PJ* (1994) Iron mobility during synmetamorphic alteration in the Selwyn Range area, NW Queensland: implications for the origin of ironstone-hosted Au-Cu deposits. Mineral Deposita 29: 250–260

*Williams PJ, Blake KL* (1993) Alteration in the Cloncurry district; roles of recognition and interpretation in exploration for Cu-Au and Pb-Zn-Ag deposits. James Cook University, Contrib Econ Geol Res Unit vol 49

*Williams PJ, Heinemann M* (1993) Maramungee; a Proterozoic Zn skarn in the Cloncurry district, Mt Isa Inlier, Queensland, Australia. Econ Geol 88: 1114–1134

*Willis IL, Brown RE, Stroud WJ, Stevens BPJ* (1983) The early Proterozoic Willyama supergroup: stratigraphic subdivision and interpretation of high to low-grade metamorphic rocks in the Broken Hill Domain, New South Wales. J Geol Soc Aust 30: 195–224

*Wingate MTD, Campbell IH, Compston W, Gibson GM* (1998) Ion microprobe U-Pb ages for Neoproterozoic basaltic magmatism in south-central Australia and implications for the breakup of Rodinia. Precamb Res 87: 135–159

*Wonder JD, Spry PG, Windom KE* (1988) Geochemistry and origin of manganese-rich rocks related to iron-formation and sulfide deposits, Western Georgia. Econ Geol 83: 1070–1081

*Yang K, Ashley PM* (1994) Stratabound breccias in the Willyama Supergroup, Olary Block, South Australia. In: Australian Research on Ore Genesis Symposium. Adelaide, Aust Min Found: 16.1–16.5

Author's addresses: *P. M. Ashley*, Division of Earth Sciences, University of New England, Armidale, New South Wales 2351, Australia; *B. G. Lottermoser*, School of Earth Sciences, James Cook University, PO Box 6811, Cairns, Queensland 4870, Australia; *J. M. Westaway*, Sons of Gwalia Limited, 16 Parliament Place, PMB 16, West Perth, WA 6872, Australia.